nature nanotechnology

ARTICLES

https://doi.org/10.1038/s41565-020-0669-6

Selective organ targeting (SORT) nanoparticles for tissue-specific mRNA delivery and CRISPR–Cas gene editing

Qiang Cheng[1,2], Tuo Wei[1,2], Lukas Farbiak[1], Lindsay T. Johnson[1], Sean A. Dilliard[1] and Daniel J. Siegwart[1]✉

CRISPR–Cas gene editing and messenger RNA-based protein replacement therapy hold tremendous potential to effectively treat disease-causing mutations with diverse cellular origin. However, it is currently impossible to rationally design nanoparticles that selectively target specific tissues. Here, we report a strategy termed selective organ targeting (SORT) wherein multiple classes of lipid nanoparticles are systematically engineered to exclusively edit extrahepatic tissues via addition of a supplemental SORT molecule. Lung-, spleen- and liver-targeted SORT lipid nanoparticles were designed to selectively edit therapeutically relevant cell types including epithelial cells, endothelial cells, B cells, T cells and hepatocytes. SORT is compatible with multiple gene editing techniques, including mRNA, Cas9 mRNA/single guide RNA and Cas9 ribonucleoprotein complexes, and is envisioned to aid the development of protein replacement and gene correction therapeutics in targeted tissues.

The development of CRISPR–Cas-based gene editing[1–3] and messenger RNA-based gene replacement technologies[4,5] have ushered in a hopeful era that promises new therapies for currently untreatable genetic diseases[6–8]. As mutated proteins are produced in specific cells, there is a critical need to develop organ-specific delivery strategies to reach the full potential of genomic medicines. Non-viral synthetic nanoparticles represent a safe and efficacious approach that allows repeated administrations. Among the available carriers, lipid nanoparticles (LNPs) represent a broad class of materials that can deliver therapeutic nucleic acids to the liver[2,4,9], including a recently US Food and Drug Administration-approved short interfering RNA LNP therapy for transthyretin-mediated amyloidosis called Onpattro[10]. Despite these advances, it is currently impossible to predictably and rationally design nanoparticles for delivery to targeted tissues beyond the liver.

We report a strategy termed Selective ORgan Targeting (SORT) that allows nanoparticles to be systematically engineered for accurate delivery of diverse cargoes including mRNA, Cas9 mRNA/single guide RNA (sgRNA) and Cas9 ribonucleoprotein (RNP) complexes to the lungs, spleens and livers of mice following intravenous (i.v.) administration (Fig. 1a). Traditional LNPs are composed of ionizable cationic lipids, amphipathic phospholipids, cholesterol and poly(ethylene glycol) (PEG) lipids. Here, we show that addition of a supplemental component (termed a SORT molecule) precisely alters the in vivo RNA delivery profile and mediates tissue-specific gene delivery and editing as a function of the percentage and biophysical property of the SORT molecule. In this work, we provide evidence for tissue-specific delivery, establish that this methodology is applicable to various nanoparticle systems and provide a new method for predictable LNP design to target therapeutically relevant cells.

Conventionally, effective intracellular delivery materials have relied on an optimal balance of ionizable amines to bind and release RNAs (pK_a between 6.0 and 6.5) and nanoparticle-stabilizing hydrophobicity[9,11–13]. This exhaustive focus on ionizable cationic lipids has produced highly effective carriers for liver hepatocytes, but has not yielded effective carriers that are capable of reaching other organs. Stimulated by our work on charge unbalanced lipids with multi-organ tropism[14], demonstration that surface charge-adjusted mRNA lipoplexes could promote delivery to dendritic cells[15] of the immune mononuclear phagocyte system (MPS) system[16,17] and other reports on non-selective delivery[18–22], we speculated that internal and/or external charge may be a key factor in tuning tissue tropism[23,24]. Therefore, in this paper, we considered if one could augment established LNP molar compositions with supplemental molecules to tune the internal charge, thereby altering the cell fate in vivo. Indeed, i.v. administration of the developed SORT LNPs enabled high levels of mRNA delivery and tissue-specific gene editing.

SORT is compatible with various methods that deploy gene editing machinery, including mRNA, Cas9 mRNA/sgRNA and Cas9 RNPs. Lung-, spleen- and liver-targeted SORT LNP delivery of Cre recombinase mRNA (Cre mRNA) to tdTomato (tdTom) mice resulted in organ-selective transfection values of: 40% of epithelial cells and 65% of endothelial cells; 12% of B cells and 10% of T cells; and 93% of hepatocytes. Lung-, spleen- and liver-targeted SORT LNPs delivered mRNAs to produce therapeutically relevant levels of proteins including human erythroprotein (hEPO), mouse interleukin-10 (IL-10) and mouse klotho (mKL). In addition, co-delivery of Cas9 mRNA and sgPCSK9 by liver SORT LNPs enabled 100% reduction of serum and protein levels of PCSK9, which is a therapeutically attractive target for treatment of cardiovascular disease[25].

Discovery and development of SORT

To examine the hypothesis that internal charge adjustment could mediate tissue-specific delivery, we conceived a strategy to add a fifth molecule to established LNP compositions with validated efficacy in liver hepatocytes. The rationale was to tune efficacious

[1]Department of Biochemistry, Simmons Comprehensive Cancer Center, The University of Texas Southwestern Medical Center, Dallas, TX, USA. [2]These authors contributed equally: Qiang Cheng, Tuo Wei. ✉e-mail: Daniel.Siegwart@UTSouthwestern.edu

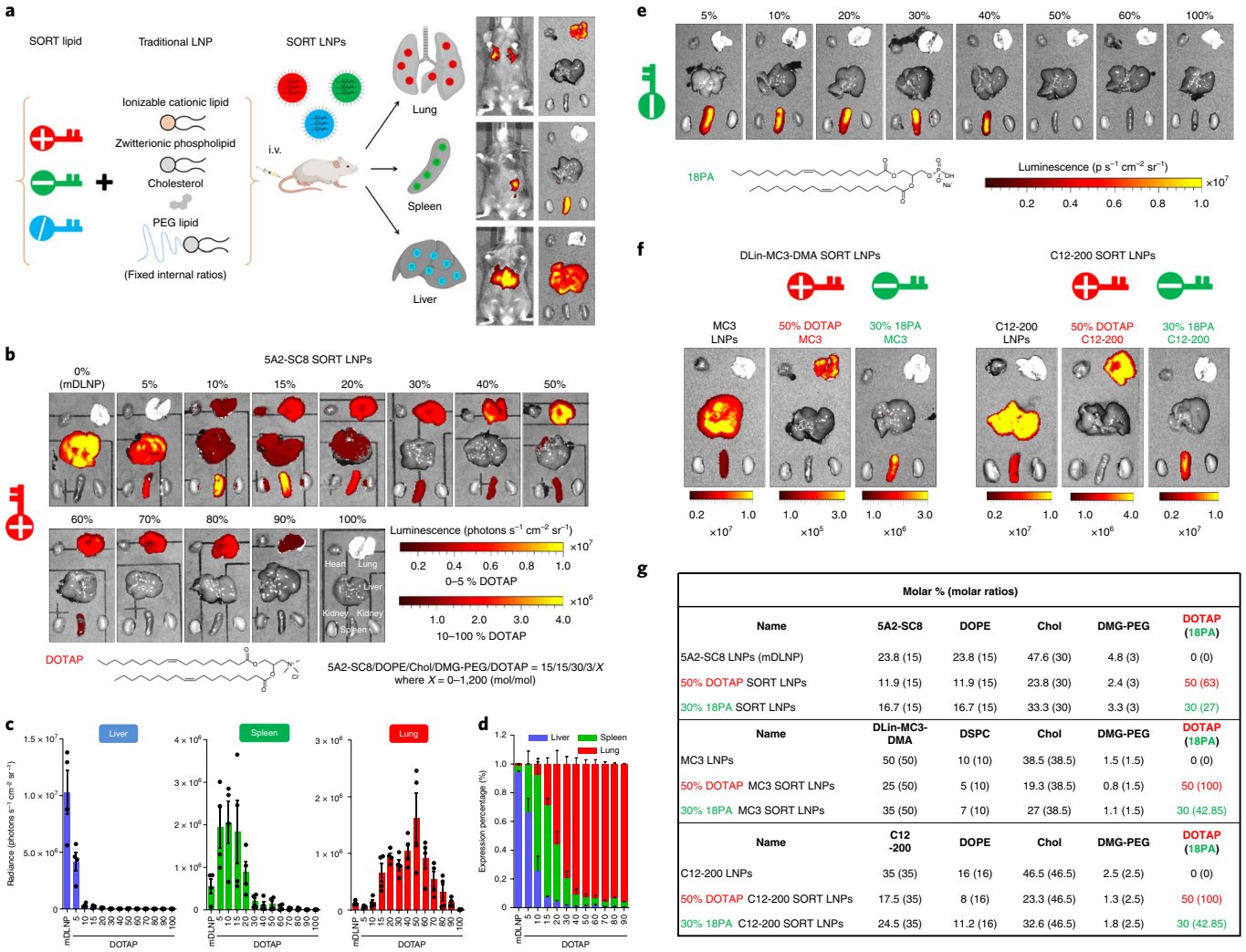

g

Molar % (molar ratios)					
Name	**5A2-SC8**	**DOPE**	**Chol**	**DMG-PEG**	**DOTAP (18PA)**
5A2-SC8 LNPs (mDLNP)	23.8 (15)	23.8 (15)	47.6 (30)	4.8 (3)	0 (0)
50% DOTAP SORT LNPs	11.9 (15)	11.9 (15)	23.8 (30)	2.4 (3)	50 (63)
30% 18PA SORT LNPs	16.7 (15)	16.7 (15)	33.3 (30)	3.3 (3)	30 (27)
Name	**DLin-MC3-DMA**	**DSPC**	**Chol**	**DMG-PEG**	**DOTAP (18PA)**
MC3 LNPs	50 (50)	10 (10)	38.5 (38.5)	1.5 (1.5)	0 (0)
50% DOTAP MC3 SORT LNPs	25 (50)	5 (10)	19.3 (38.5)	0.8 (1.5)	50 (100)
30% 18PA MC3 SORT LNPs	35 (50)	7 (10)	27 (38.5)	1.1 (1.5)	30 (42.85)
Name	**C12-200**	**DOPE**	**Chol**	**DMG-PEG**	**DOTAP (18PA)**
C12-200 LNPs	35 (35)	16 (16)	46.5 (46.5)	2.5 (2.5)	0 (0)
50% DOTAP C12-200 SORT LNPs	17.5 (35)	8 (16)	23.3 (46.5)	1.3 (2.5)	50 (100)
30% 18PA C12-200 SORT LNPs	24.5 (35)	11.2 (16)	32.6 (46.5)	1.8 (2.5)	30 (42.85)

Fig. 1 | SORT allows LNPs to be systematically and predictably engineered to accurately deliver mRNA into specific organs. a, Addition of a supplemental component (termed a SORT molecule) to traditional LNPs systematically alters the in vivo delivery profile and mediates tissue-specific delivery as a function of the percentage and biophysical property of the SORT molecule. This methodology successfully redirected multiple classes of nanoparticles. **b**, 5A2-SC8 SORT LNPs were formulated as indicated to produce a series of LNPs with 0% to 100% SORT lipid (fraction of total lipids). Here, inclusion of a permanently cationic lipid (DOTAP) systematically shifted luciferase protein expression, from liver to spleen to lung, as a function of DOTAP percentage. **c**, Quantification data demonstrated that SORT molecule percentage is the most important factor for tissue-specific delivery. Data are shown as mean ± s.e.m. ($n = 4$ biologically independent animals). **d**, Relative luciferase expression in each organ demonstrated that fractional expression could be predictably tuned (0.1 mg kg^{-1} Luc mRNA, i.v., 6 h). Data are shown as mean ± s.e.m. ($n = 4$ biologically independent animals). **e**, Inclusion of an anionic SORT molecule enabled selective mRNA delivery to the spleen. Luciferase expression was only observed in the spleen when 18PA lipid was introduced into mDLNPs up to 40%. **f**, Ex vivo images of luminescence in major organs of DLin-MC3-DMA SORT LNPs and C12-200 SORT LNPs (0.1 Luc mRNA mg kg^{-1}, i.v., 6 h). **g**, Formulation details of selected SORT molecules.

LNP formulations without destroying the core four-component ratios that are essential for mediating RNA encapsulation and endosomal escape[26,27].

We first examined the effect of adding a permanently cationic lipid (defined as positively charged without pK_a or p$K_a > 8$) to a degradable dendrimer ionizable (p$K_a < 8$) cationic lipid 5A2-SC8 formulation named mDLNPs[28–30], which effectively delivered fumarylacetoacetate hydrolase (FAH) mRNA to liver hepatocytes and extended survival in FAH-knockout mice[27]. This initial base mDLNP formulation consisted of 5A2-SC8, 1,2-dioleoyl-*sn*-glycero-3-phosphoethanolamine (DOPE), cholesterol, 1,2-dimyristoyl-*rac*-glycerol-methoxy(poly(ethylene glycol)) (DMG-PEG; 15/15/30/3, mol/mol) and mRNA (5A2-SC8/mRNA, 20/1, wt/wt) (Supplementary Fig. 1). We then formed a series of LNPs by systematically increasing the percentage of additional permanently cationic lipid from 5 to 100% of the total lipids (Fig. 1b and Supplementary Fig. 1). Herein, we focused on lipids acting as SORT molecules to aid self-assembly, initially selecting 1,2-dioleoyl-3-trimethylammonium-propane (DOTAP) because it is a well-known quaternary amino lipid, and prepared a titrated series of five-component formulations (Supplementary Fig. 1).

We then evaluated the effects of SORT modification by delivering i.v. luciferase (Luc) mRNA at a dose of 0.1 mg kg^{-1}. Surprisingly, with an increasing molar percentage of DOTAP, the resulting luciferase protein expression moved progressively from liver to spleen, and then to lung, demonstrating a clear and precise organ-specific delivery trend with a threshold that allowed exclusive lung delivery (Fig. 1b). The DOTAP percentage was the key factor for tuning tissue specificity. Base mDLNPs (0% DOTAP) were optimal for liver delivery, which was anticipated as they had been previously

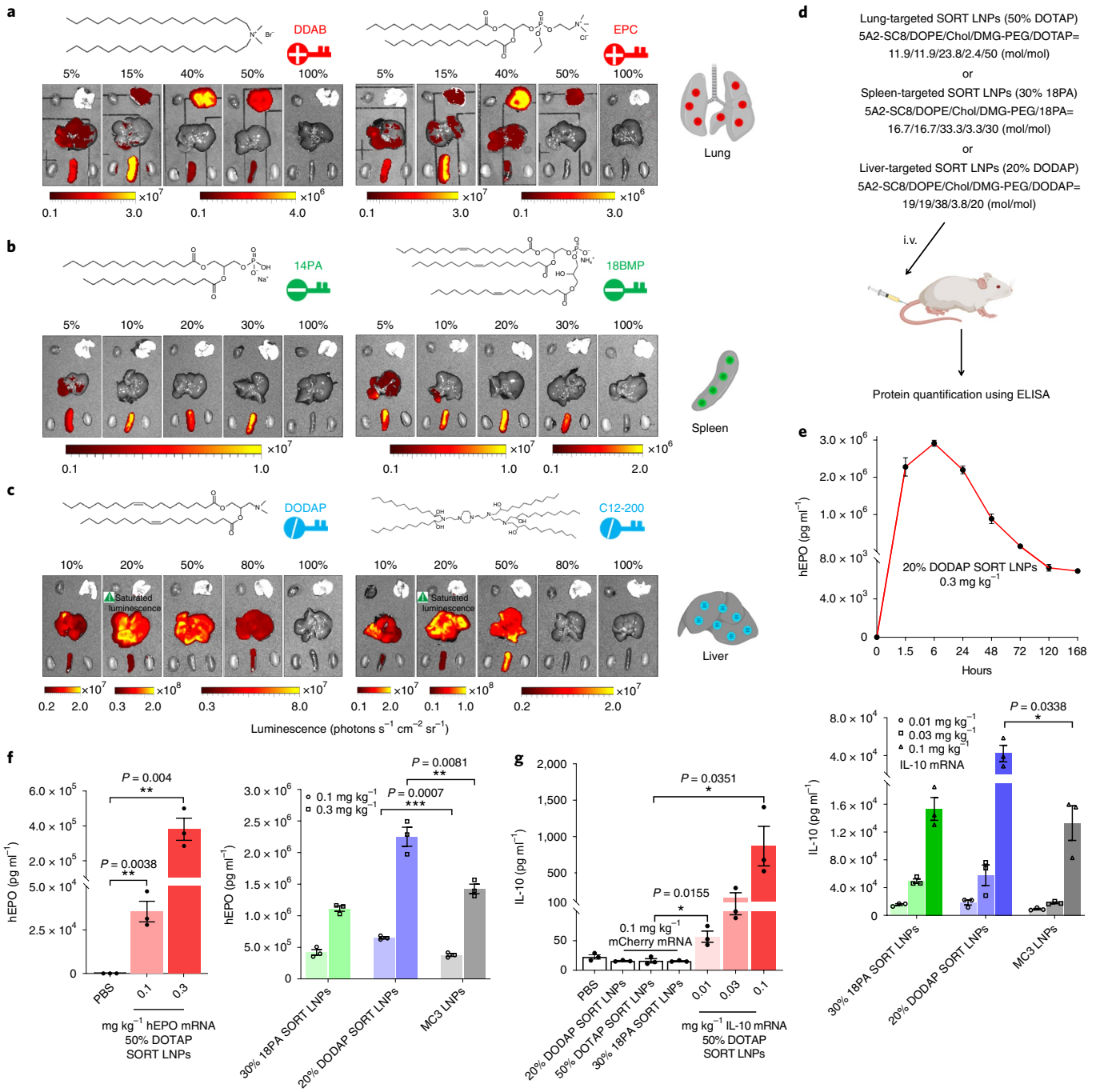

Fig. 2 | SORT relies on general biophysical properties and not exact chemical structures to deliver mRNAs encoding for therapeutically relevant proteins. a, SORT molecules could be divided into specific groups with defined biophysical properties. Permanently cationic SORT lipids (DDAB, EPC and DOTAP) all resulted in the same mRNA delivery profile. **b**, Anionic SORT lipids (14PA, 18BMP, 18PA) all resulted in the same mRNA delivery profile. **c**, Ionizable cationic SORT lipids with tertiary amino groups (DODAP, C12-200) enhanced liver delivery without luciferase expression in the lungs (0.1 mg kg^{-1}, 6 h). **d**, Scheme for mRNA delivery of secreted proteins. **e**, High levels of hEPO expression persisted for more than 1 week following administration of 0.3 mg kg^{-1} hEPO mRNA in 20% DODAP SORT LNPs. Data are presented as mean ± s.e.m. ($n = 3$ biologically independent animals). **f**, hEPO was quantified using an ELISA assay in serum following i.v. administration of hEPO mRNA in lung-, spleen- and liver-targeted SORT LNPs, and MC3 LNPs. Data are presented as mean ± s.e.m. ($n = 3$ biologically independent animals). **g**, IL-10 was quantified using an ELISA assay in serum following i.v. administration of mouse IL-10 mRNA in lung-, spleen- and liver-targeted SORT LNPs, and MC3 LNPs. mCherry mRNA SORT formulations and PBS were used as controls. Data are presented as mean ± s.e.m. ($n = 3$ biologically independent animals). A two-tailed unpaired *t*-test was used to determine the significance of the comparisons of data indicated in **f** and **g** (*$P < 0.05$; **$P < 0.01$; ***$P < 0.001$; ****$P < 0.0001$).

optimized for hepatocyte delivery[27]; 10–15% aided spleen delivery, and 50% was optimal for lung delivery, albeit with some reduction in activity (Fig. 1c). We note that the efficacy of in vitro and in vivo delivery did not correlate (Supplementary Fig. 2), demonstrating that LNPs with high in vivo efficacy may be missed in traditional in vitro assay screens that do not capture the organism-level biology

of specific cells in various organs. This provides one explanation for why the discovery of predictable organ-specific delivery has been so elusive. On calculating the relative expression in each organ, we found that SORT completely altered delivery from the liver to the lungs (Fig. 1d and Supplementary Fig. 3).

With the functional role of the permanently cationic SORT lipid explained, we then hypothesized that inclusion of other molecules may also alter tissue tropism. To explore this hypothesis, negatively charged 1,2-dioleoyl-*sn*-glycero-3-phosphate (18PA) was incorporated as a SORT molecule in a similar manner to DOTAP (Supplementary Fig. 1). At an 18PA incorporation of 10–40%, SORT LNPs now mediated completely selective delivery to the spleen with no luciferase expression in any other organs (Fig. 1e). Thus, negatively charged SORT lipids allow for explicit delivery to the spleen. These results indicated that SORT molecule chemistry and percentage can be tailored for tissue-specific delivery via i.v. injection.

SORT is generally applicable to LNP type and molecular class

We next asked if the SORT methodology could be applied to other classes of established four-component LNPs. First, DLin-MC3-DMA was formulated with 1,2-distearoyl-*sn*-glycero-3-phosphocholine (DSPC), cholesterol and DMG-PEG with the same molar composition of lipids used in the US Food and Drug Administration-approved Onpattro (Patisiran) formulation[31] (Supplementary Fig. 4). This formulation has been established as a benchmark for both short interfering RNA[11] and mRNA[32–34] delivery. To date, DLin-MC3-DMA LNPs have only delivered RNA to the liver following i.v. administration, which we confirmed (Fig. 1f). As expected, supplementing DLin-MC3-DMA LNPs with DOTAP altered the protein expression profile from the liver to spleen to lung, mirroring the results of 5A2-SC8 SORT LNPs. To study this further, we incorporated DOTAP into C12-200 lipid-like LNPs (LLNPs) (Fig. 1g and Supplementary Fig. 4), which are also validated for RNA delivery to the liver[35,36], and observed an identical trend (Fig. 1f and Supplementary Fig. 4). Additionally, the inclusion of 18PA as a SORT molecule mirrored our results for 5A2-SC8 and mediated exclusive delivery of Luc mRNA to the spleen for both DLin-MC3-DMA and C12-200 LNPs (Fig. 1f,g). DLin-MC3-DMA is a two-tailed lipid with a single dimethylamine headgroup that forms stable nucleic acid LNPs, while C12-200 is a representative lipidoid that forms LLNPs. Thus, we show that the SORT methodology is generally applicable to other classes of ionizable cationic lipid LNPs, which will allow existing liver-targeting LNPs to be tuned to deliver mRNA to the spleen or lungs. Specifically, the SORT technology may allow rapid redevelopment of preclinical and clinical liver-targeting LNPs for the treatment of diseases of the lung and spleen.

To understand whether the tissue tropism profiles observed are specific to exact chemical structures or are applicable to defined chemical classes, we evaluated multiple permanently cationic, anionic, zwitterionic, and ionizable cationic SORT lipids (Fig. 2 and Supplementary Table 1). First, we generated 5A2-SC8 SORT LNPs with two additional permanently cationic lipids: dimethyldioctadecylammonium (DDAB) and 1,2-dimyristoyl-*sn*-glycero-3-ethylphosphocholine (EPC). These lipids all contain quaternary amino groups, but there are major chemical differences in the polar headgroup, linker region and hydrophobic domain (for example, degree of saturation). LNPs containing 5, 15, 40, 50, and 100% DDAB or EPC were formulated and characterized. Importantly, the in vivo luciferase expression profile matched that of the DOTAP LNPs, where the luminescence activity systematically shifted from the liver to spleen, and then to the lung with increasing DDAB or EPC percentages (Fig. 2a). We next examined 1,2-dimyristoyl-*sn*-glycero-3-phosphate (14PA) and *sn*-(3-oleoyl-2-hydroxy)-glycerol-1-phospho-sn-3'-(1',2'-dioleoyl)-glycerol (18BMP) as representative anionic lipids with very different structures. All the anionic SORT lipids promoted exclusive delivery to the spleen (Fig. 2b). This design flexibility provides a pathway for the optimization of future SORT molecules to balance potency, selectivity, and tolerability.

Inspired by these findings, we then considered what would happen if other ionizable cationic lipids were added to established formulations. As expected, the addition of 1,2-dioleoyl-3-dimethylammonium-propane (DODAP) or C12-200 to 5A2-SC8 mDL-NPs did not significantly alter tissue tropism, but surprisingly did enhance liver delivery >tenfold at 20% incorporation (Fig. 2c). Interestingly, simply supplementing already established mDL-NPs with additional 5A2-SC8 as a SORT molecule dramatically improved liver mRNA delivery, producing 10^7 photons s^{-1} cm^{-2} at the low dose of 0.05 mg kg^{-1}. Thus, SORT offers a new strategy to further improve liver-targeting LNP systems (Supplementary Fig. 5). We also evaluated the effect of using zwitterionic lipids (2-((2,3-bis(oleoyloxy)propyl)dimethylammonio)ethyl ethyl phosphate (DOCPe) and DSPC) as SORT molecules. While we found that the tissue tropism moved from liver to spleen, it was not as selective compared to the use of cationic or anionic SORT lipids (Supplementary Fig. 6).

To test the limits of the SORT methodology, we examined if SORT could 'activate' otherwise inactive formulations. In fact, supplementing a completely inactive formulation with DODAP or DOTAP resulted in tissue-specific delivery to the spleen and lung (Supplementary Fig. 7). We note that all the SORT LNPs still contained ionizable cationic lipids, which are considered essential for endosomal escape[26] due to their ability to acquire charge. We performed control experiments and confirmed that inclusion of an ionizable cationic lipid was needed for efficacy (Supplementary Fig. 8). Taking all of these results together, we conclude that SORT is a modular and general strategy to achieve tissue-targeted delivery.

This led to the selection of lung-, spleen- and liver-targeted 5A2-SC8 SORT LNPs (Fig. 2d). We confirmed that Luc delivery was dose-responsive (Supplementary Fig. 9). We also verified that SORT-enabled tissue specificity occurs quickly and is not dependent on time (Supplementary Fig. 10). We analysed the tissue-specific mRNA delivery more precisely by homogenizing isolated tissues to quantify luminescence normalized to the tissue weight and total protein for each organ (Supplementary Fig. 11). Considering potential therapeutic applications, formulation stability was monitored over time, which revealed that SORT LNPs maintained physiochemical properties and in vivo delivery efficacy after storage at 4 °C (Supplementary Fig. 12).

Next, we evaluated the ability of these formulations to deliver mRNAs encoding secreted therapeutic proteins: hEPO, IL-10 and mKL. This approach allowed us to quantify protein concentrations in serum to directly test all organ-specific SORT LNPs (Fig. 2d). hEPO production following i.v. administration of 20% DODAP liver SORT LNPs peaked at 6 h and was maintained for more than 1 week (Fig. 2e and Supplementary Fig. 13). All three tissue-specific formulations mediated high levels of protein production at low mRNA doses for both hEPO mRNA (0.1 and 0.3 mg kg^{-1}) and IL-10 mRNA (0.01 mg kg^{-1} to 0.1 mg kg^{-1}) in a dose-responsive manner (Fig. 2f,g). Similar delivery trends were observed for mKL mRNA (Supplementary Fig. 13). We next evaluated in vivo toxicity using a higher dose than needed to produce therapeutically relevant protein levels in the blood. SORT LNPs with single or multiple dosing did not alter kidney and liver function and serum cytokines (Supplementary Fig. 14), and no adverse signs of injury in tissue histology (Supplementary Fig. 15) were observed at the tested dose (1 mg kg^{-1} mRNA). These results suggest that SORT LNPs are well tolerated and mediate therapeutically relevant levels of protein production.

SORT enables delivery to therapeutically relevant cell types

Given the ability of SORT LNPs to target specific organs, we applied our findings to tissue-specific gene editing via i.v. injection. CRISPR–Cas technology[6–8] can edit the genome in a precise and

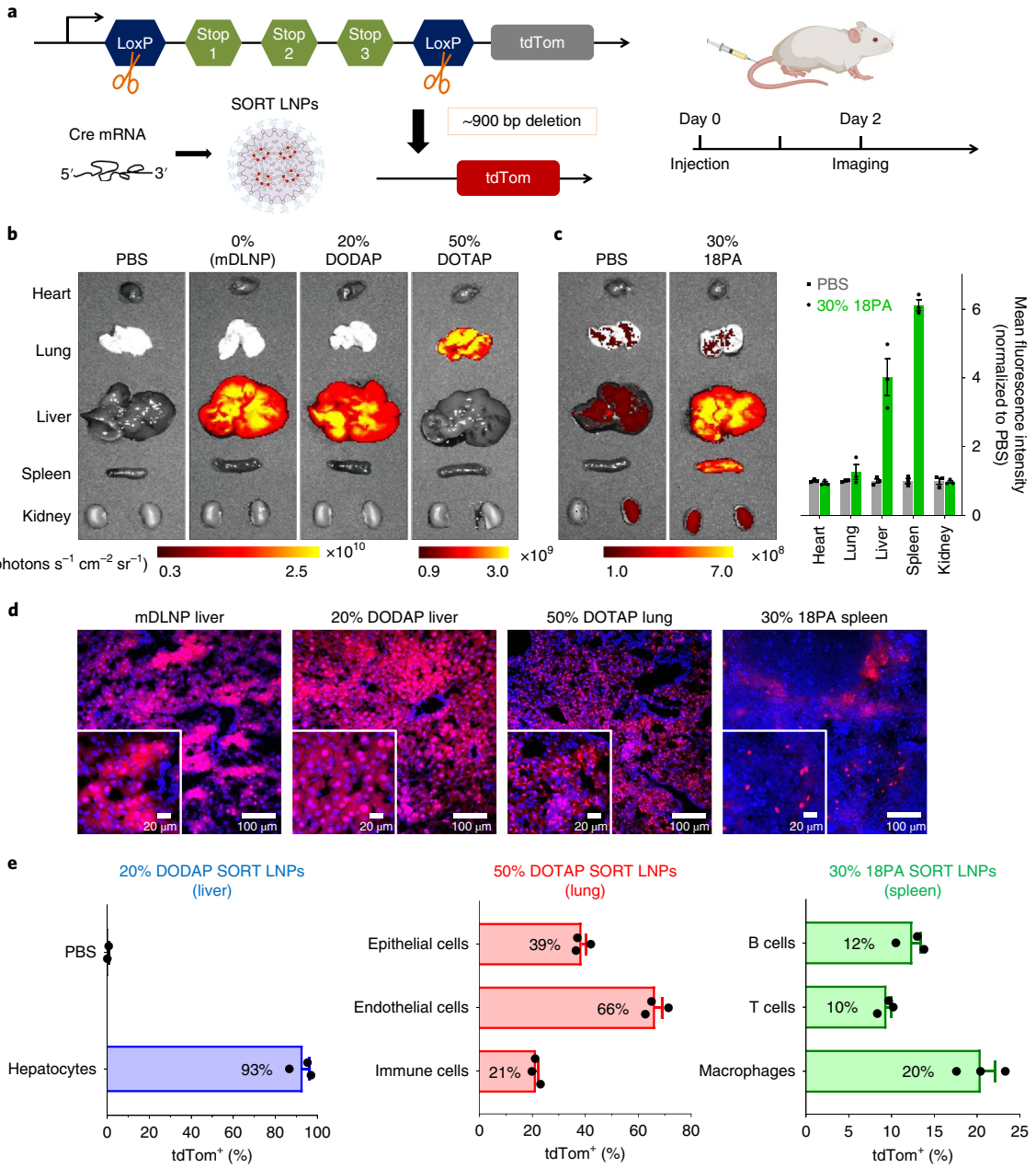

Fig. 3 | SORT LNPs enabled tissue-specific tdTom activation by Cre mRNA delivery. a, The schematic illustration shows that delivery of Cre mRNA activates tdTom expression in tdTom transgenic mice via Cre-mediated genetic deletion of the stop cassette. **b**, mDLNP and liver-targeted SORT LNPs (20% DODAP) induced tdTom fluorescence specifically in the liver and lung-targeted SORT LNPs (50% DOTAP) selectively edited the lung. tdTom fluorescence in the main organs was detected 2 d after i.v. injection of Cre mRNA-loaded LNPs ($n = 3$ biologically independent animals). **c**, Spleen-targeted SORT LNPs (30% 18PA) induced gene editing in the spleen (note high liver background fluorescence in PBS injected mice). Data are presented as mean ± s.e.m. ($n = 3$ biologically independent animals). **d**, Confocal microscopy was employed to further verify effective tissue editing ($n = 3$ biologically independent animals). **e**, FACS was used to quantify the percentage of tdTom$^+$ cells within defined cell type populations of the liver, lung and spleen (0.3 mg kg^{-1}, day 2). Data are presented as mean ± s.e.m. ($n = 3$ biologically independent animals).

sequence-dependent manner and has been rapidly developed for use in diverse applications, including the correction of disease-causing mutations[37–41]. Gene editing can be achieved by local administration[42–44]. However, many serious genetic disorders arise from mutations in cells deep in organs, where correction of specific cells will be required to cure disease. Such correction may be best achieved by systemic administration. We, and others, recently reported that i.v. co-delivery of Cas9 mRNA and sgRNA is a safe and effective strategy to enable gene editing[14,39,45]. To our knowledge, however, up to now there have been no reports of LNPs rationally engineered to edit cells in organs outside of the liver.

To examine and quantify the ability of SORT LNPs to mediate organ-specific gene editing, we utilized genetically engineered tdTom reporter mice containing a LoxP flanked stop cassette[46] that prevents expression of the tdTom protein[44]. Once the stop cassette is deleted, tdTom fluorescence is turned on, allowing detection of gene edited cells (Fig. 3a). We initially delivered Cre mRNA, which produces the Cre protein and deletes the stop to activate tdTom in

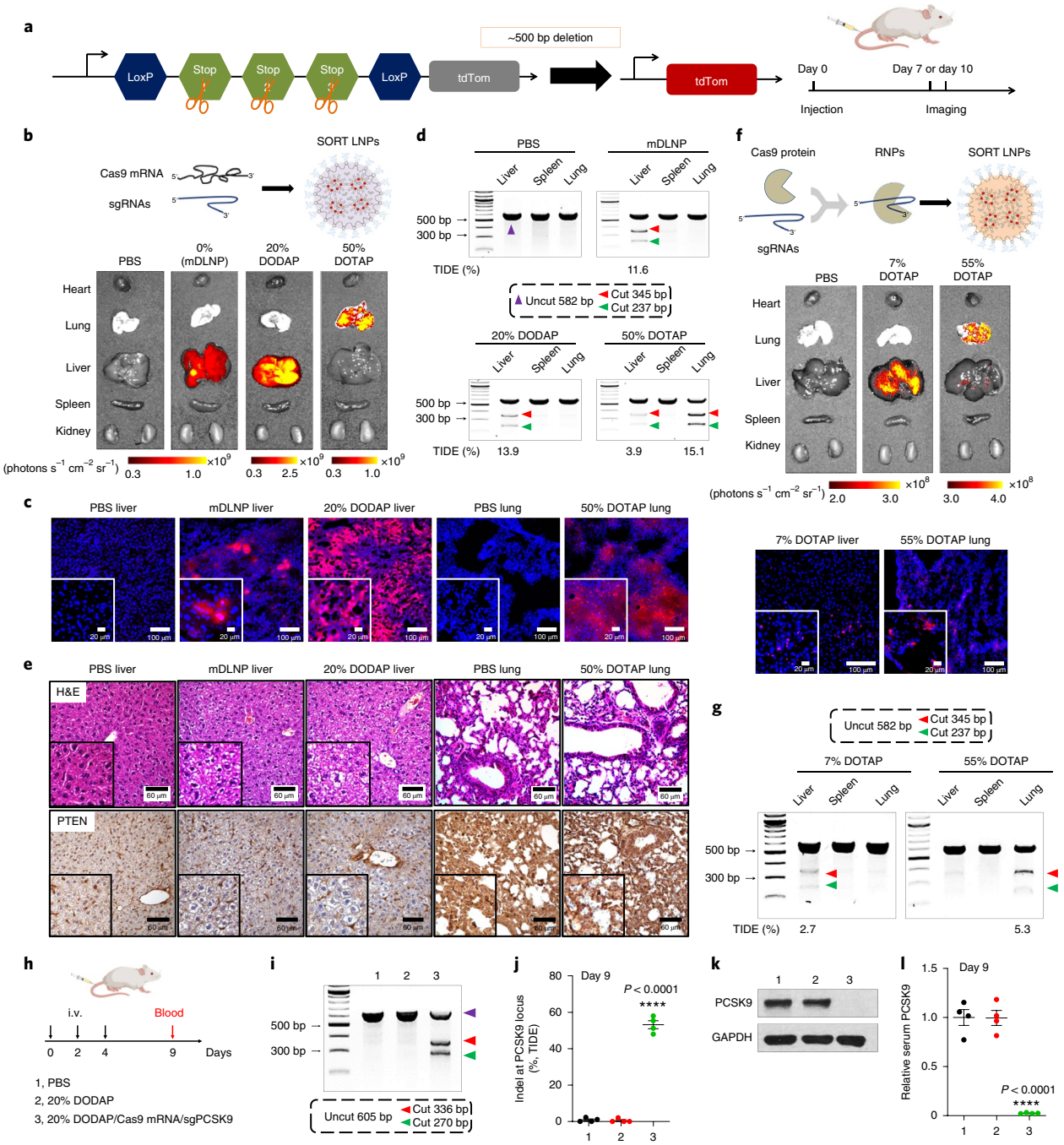

Fig. 4 | SORT LNPs mediated tissue-specific CRISPR–Cas gene editing of tdTom transgenic mice and C57/BL6 wild-type mice by delivering Cas9 RNPs and co-delivering Cas9 mRNA and sgRNA. a, The schematic illustration shows that co-delivery of Cas9 mRNA (or Cas9 protein) and sgTom1 activates tdTom expression in tdTom transgenic mice. **b**, mDLNP and SORT LNPs (20% DODAP) induced tdTom fluorescence specifically in the liver and SORT LNPs (50% DOTAP) selectively edited the lung with a 2.5 mg kg^{-1} dose (Cas9 mRNA/sgTom1, 4/1, wt/wt; measured on day 10, $n = 3$ biologically independent animals). **c**, tdTom expression was confirmed by confocal imaging of tissue sections ($n = 3$ biologically independent animals). **d**, Cas9 mRNA and sgPTEN were co-delivered in SORT LNPs to selectively edit the liver, lung and spleen of C57/BL6 mice with 2.5 mg kg^{-1} total mRNA (Cas9 mRNA/sgPTEN, 4/1, wt/wt; measured on day 10, $n = 3$ biologically independent animals). The T7E1 assay indicated that tissue-specific PTEN editing was achieved. Editing was quantified using DNA sequencing and TIDE analysis. **e**, H&E sections and IHC further confirmed successful PTEN editing ($n = 3$ biologically independent animals). Clear cytoplasm indicated lipid accumulation in H&E sections and PTEN loss in IHC images. **f**, Delivery of Cas9/sgTom1 RNP complexes in 7% DOTAP or 55% DOTAP SORT LNPs induced tdTom fluorescence specifically in the liver and lungs, respectively (1.5 mg kg^{-1} sgTom1, measured on day 7, $n = 3$ biologically independent animals). tdTom expression was confirmed by confocal imaging of tissue sections. **g**, Liver- and lung-tropic SORT LNPs also delivered Cas9/sgPTEN RNPs to selectively edit the liver and lungs in C57/BL6 mice (1.5 mg kg^{-1} sgPTEN, measured on day 7, $n = 3$ biologically independent animals). The T7E1 and TIDE assays indicated that tissue-specific PTEN editing was achieved. **h**, Co-delivery of Cas9 mRNA and modified sgPCSK9 was achieved with 20% DODAP SORT LNPs in C57BL/6 mice via three i.v. injections (days 0, 2, 4) ($n = 4$ biologically independent animals). **i**–**l**, At day 9, ~60% indel at the PCSK9 locus of liver tissue was quantified using T7E1 assay (**i**) and TIDE analysis (**j**), which resulted in ~100% PCSK9 protein reduction in liver tissue (western blot) (**k**) and serum (ELISA) (**l**). The results of **h**–**l** were obtained from four biologically independent animals. Data of **j** and **l** are presented as mean ± s.e.m. A two-tailed unpaired *t*-test was used to determine the significance of the comparisons of data indicated in **j** and **l** (*$P < 0.05$; **$P < 0.01$; ***$P < 0.001$; ****$P < 0.0001$).

edited cells. Fluorescent tissues were readily apparent (Fig. 3b) in the selected organs treated with liver-, lung- and spleen-targeted SORT LNPs. We note that these mice have weaker background organ autofluorescence in the spleen compared to other organs, which required the use of separate controls (Fig. 3c and Supplementary Fig. 16). This makes the detection of spleen specificity more challenging; nevertheless, tdTom positive cells were easily seen using confocal imaging of tissue sections (Fig. 3d).

To gain an initial estimate of the cell types amenable to delivery by SORT LNPs, we quantified delivery to specific cell types within the liver, lung and spleen using flow cytometry of cells extracted from edited organs following delivery of Cre mRNA (Fig. 3e). Liver-targeted SORT LNPs (20% DODAP) delivered Cre mRNA to ~93% of all hepatocytes in the liver following a single injection of 0.3 mg kg^{-1} Cre mRNA (Fig. 3e and Supplementary Fig. 17). Lung-targeted SORT LNPs (50% DOTAP) transfected ~40% of all epithelial cells, ~65% of all endothelial cells and ~20% of immune cells in the lungs at the same dose (Fig. 3e and Supplementary Fig. 18). Given that epithelial cells are a primary target for correction of mutations in the cystic fibrosis transmembrane conductance regulator (CFTR) that causes cystic fibrosis, this result establishes lung-targeted SORT LNPs as a compelling delivery system with immediate application for correcting CFTR mutations. Finally, spleen-targeted SORT LNPs (30% 18PA) transfected ~12% of all B cells, ~10% of all T cells, and ~20% of all macrophages (Fig. 3e and Supplementary Fig. 19). Due to the improved selectivity, spleen-targeted SORT LNPs could be applicable in treating non-Hodgkin's B-cell lymphoma and other immune disorders. Although our initial focus was on single, low-dose injection quantification, we note that higher levels of transfection are achievable by administering higher doses or multiple injections.

SORT allows tissue-specific gene editing

Next, we examined the ability of SORT LNPs to achieve tissue-specific CRISPR–Cas gene editing via i.v. co-delivery of Cas9 mRNA and sgRNA in a single nanoparticle (Fig. 4a, Supplementary Fig. 20 and Supplementary Table 2). We injected liver and lung-targeting SORT LNPs at a dose of 2.5 mg kg^{-1} total RNA (4/1 mRNA/sgRNA, wt/wt) and quantified gene editing 10 d after a single i.v. injection. As shown in Fig. 4b, strong tdTom fluorescence was observed in the liver for both mDLNP- and 20% DODAP SORT LNP-treated mice, and in the lung of 50% DOTAP SORT LNP-treated mice. The fluorescence was then confirmed by imaging tissue sections using confocal microscopy (Fig. 4c). All the results were consistent with the Luc mRNA delivery results. Due to the fast turnover of splenic immune cells in mice[47], we optimized the weight ratio of Cas9/sgRNA at 2/1 (Supplementary Fig. 21) and tested the spleen editing 2 d after injection. Accounting for background autofluorescence, bright tdTom fluorescence was observed in the spleen of 30% 18PA-treated mice (Supplementary Fig. 22). Next, we focused on direct delivery of Cas9 RNPs, which is the most challenging strategy for synthetic carriers. The use of permanently cationic SORT lipids enabled Cas9 protein/sgTom1 complexes to be encapsulated with control over tissue tropism. I.v. injection of 7% DOTAP SORT LNPs enabled liver editing, while 55% DOTAP SORT LNPs enabled exclusive lung editing (Fig. 4f). These data indicate that the described methodology enables liver-, lung- and spleen-targeted CRISPR–Cas gene editing.

To expand beyond reporter mice, we tested the ability of tissue-specific LNPs to edit an endogenous target. We selected phosphatase and tensin homolog (PTEN) because it is a well-established tumour suppressor expressed in most cells. Wild-type C57BL/6 mice were injected with SORT LNPs co-loaded with Cas9 mRNA and sgPTEN (2.5 mg kg^{-1} total RNA). Generation of insertions and deletions (indels) was quantified 10 d after a single i.v. injection. As shown in Fig. 4d, clear DNA cleavage bands were observed in specific tissues following the T7E1 assay, which demonstrated that both base mDLNPs (11.6% indels confirmed using TIDE analysis) and 20% DODAP SORT LNPs (13.9%) mediated effective PTEN editing in liver, but not at all in the lung or spleen. Remarkably, 50% DOTAP SORT LNPs (15.1%) showed PTEN editing exclusively in the lungs. To further confirm PTEN editing, haematoxylin and eosin (H&E) staining and immunohistochemistry (IHC) of tissue sections was performed. As shown in Fig. 4e, cells in tissue sections obviously displayed clear cytoplasm, which is a known phenotype of PTEN loss due to lipid accumulation[48]. Moreover, negative staining of PTEN was observed in IHC sections in both liver and lung tissues. Although it was more challenging to distinguish spleen-targeting 18PA SORT LNP editing in the tdTom mouse model, clear spleen PTEN editing could be observed in wild-type mice (Supplementary Fig. 22). Next, we applied SORT to Cas9 RNPs and examined the endogenous editing of PTEN. As before, 7% and 55% DOTAP SORT LNPs containing Cas9 protein/sgPTEN enabled liver (2.7%) and lung (5.3%) specific editing, respectively (Fig. 4g). We also evaluated the off-target effects for PTEN and did not detect any off-target DNA editing (Supplementary Figs. 23 and 24).

Finally, to establish that SORT LNPs can edit therapeutically relevant targets at significant levels, we co-delivered Cas9 mRNA and an sgRNA targeting PCSK9 (Fig. 4h), a highly attractive target for familial hypercholesterolaemia and atherosclerotic cardiovascular disease[25]. We found that 20% DODAP SORT LNPs were able to significantly induce indels at the PCSK9 locus (~60% confirmed using TIDE) (Fig. 4i,j and Supplementary Fig. 25), leading to an ~100% reduction in PCSK9 protein levels in the liver (Fig. 4k and Supplementary Fig. 25) and serum (Fig. 4l and Supplementary Fig. 25). We also observed a higher liver-to-body weight ratio, which demonstrated a clear phenotypic change due to lipid accumulation in the liver after PCSK9 knockout (Supplementary Fig. 25). The results provided by targeting endogenous genes demonstrate that rationally guided tissue-selective gene editing can be achieved using synthetic carriers.

Conclusions

The discovery of SORT, which allows predictable nanoparticle delivery of RNA to specific organs, is anticipated to aid the development of protein replacement and gene correction therapeutics. As delivery efficacy is strongly correlated to modular molecular class, we believe this methodology can be widely applied to existing LNPs and other nanoparticle systems. We speculate that SORT may allow the rational design of carriers for a variety of cargoes (including proteins and other drugs) and organs. Our current research is focused on determining the precise mechanisms that explain how SORT enables tissue targeting. Although more work remains, initial data indicates that inclusion of SORT molecules alters the biodistribution of SORT LNPs to different tissues, changes the global apparent pK_a values[11] and endows distinct protein coronas[49,50]. The results of these investigations will be published in a future manuscript. Nevertheless, the current data disclosing the high degree of editing in specific cells positions the discovery of SORT LNPs to treat an array of diseases in a highly accurate manner. Thus, it is anticipated that SORT may open new avenues of development for gene correction therapeutics.

Online content

Any methods, additional references, Nature Research reporting summaries, source data, extended data, supplementary information, acknowledgements, peer review information; details of author contributions and competing interests; and statements of data and code availability are available at https://doi.org/10.1038/s41565-020-0669-6.

Received: 4 December 2019; Accepted: 19 February 2020;
Published online: 6 April 2020

References

1. Doudna, J. A. & Charpentier, E. Genome editing: the new frontier of genome engineering with CRISPR-Cas9. *Science* **346**, 1258096 (2014).
2. Wang, H. X. et al. CRISPR/Cas9-based genome editing for disease modeling and therapy: challenges and opportunities for nonviral delivery. *Chem. Rev.* **117**, 9874–9906 (2017).
3. Sander, J. D. & Joung, J. K. CRISPR–Cas systems for editing, regulating and targeting genomes. *Nat. Biotechnol.* **32**, 347–355 (2014).
4. Hajj, K. A. & Whitehead, K. A. Tools for translation: non-viral materials for therapeutic mRNA delivery. *Nat. Rev. Mater.* **2**, 17056 (2017).
5. Sahin, U., Kariko, K. & Tureci, O. mRNA-based therapeutics: developing a new class of drugs. *Nat. Rev. Drug Discov.* **13**, 759–780 (2014).
6. Jinek, M. et al. A programmable dual-RNA-guided DNA endonuclease in adaptive bacterial immunity. *Science* **337**, 816–821 (2012).
7. Cong, L. et al. Multiplex genome engineering using CRISPR/Cas systems. *Science* **339**, 819–823 (2013).
8. Mali, P. et al. RNA-guided human genome engineering via Cas9. *Science* **339**, 823–826 (2013).
9. Kanasty, R., Dorkin, J. R., Vegas, A. & Anderson, D. Delivery materials for siRNA therapeutics. *Nat. Mater.* **12**, 967–977 (2013).
10. Wood, H. FDA approves patisiran to treat hereditary transthyretin amyloidosis. *Nat. Rev. Neurol.* **14**, 570 (2018).
11. Jayaraman, M. et al. Maximizing the potency of siRNA lipid nanoparticles for hepatic gene silencing in vivo. *Angew. Chem. Int. Ed.* **51**, 8529–8533 (2012).
12. Nelson, C. E. et al. Balancing cationic and hydrophobic content of PEGylated siRNA polyplexes enhances endosome escape, stability, blood circulation time, and bioactivity in vivo. *ACS Nano* **7**, 8870–8880 (2013).
13. Hao, J. et al. Rapid synthesis of a lipocationic polyester library via ring-opening polymerization of functional valerolactones for efficacious siRNA delivery. *J. Am. Chem. Soc.* **137**, 9206–9209 (2015).
14. Miller, J. B. et al. Non-viral CRISPR/Cas gene editing in vitro and in vivo enabled by synthetic nanoparticle co-delivery of Cas9 mRNA and sgRNA. *Angew. Chem. Int. Ed.* **56**, 1059–1063 (2017).
15. Kranz, L. M. et al. Systemic RNA delivery to dendritic cells exploits antiviral defence for cancer immunotherapy. *Nature* **534**, 396–401 (2016).
16. Wilhelm, S. et al. Analysis of nanoparticle delivery to tumours. *Nat. Rev. Mater.* **1**, 16014 (2016).
17. Gustafson, H. H., Holt-Casper, D., Grainger, D. W. & Ghandehari, H. Nanoparticle uptake: the phagocyte problem. *Nano Today* **10**, 487–510 (2015).
18. Fehring, V. et al. Delivery of therapeutic siRNA to the lung endothelium via novel lipoplex formulation DACC. *Mol. Ther.* **22**, 811–820 (2014).
19. Dahlman, J. E. et al. In vivo endothelial siRNA delivery using polymeric nanoparticles with low molecular weight. *Nat. Nanotechnol.* **9**, 648–655 (2014).
20. Fenton, O. S. et al. Synthesis and biological evaluation of ionizable lipid materials for the in vivo delivery of messenger RNA to B lymphocytes. *Adv. Mater.* **29**, 1606944 (2017).
21. Kowalski, P. S. et al. Ionizable amino-polyesters synthesized via ring opening polymerization of tertiary amino-alcohols for tissue selective mRNA delivery. *Adv. Mater.* **30**, e1801151 (2018).
22. Sago, C. D. et al. High-throughput in vivo screen of functional mRNA delivery identifies nanoparticles for endothelial cell gene editing. *Proc. Natl Acad. Sci. USA* **115**, E9944–E9952 (2018).
23. Kaczmarek, J. C. et al. Polymer-lipid nanoparticles for systemic delivery of mRNA to the lungs. *Angew. Chem. Int. Ed.* **55**, 13808–13812 (2016).
24. Yan, Y., Xiong, H., Zhang, X., Cheng, Q. & Siegwart, D. J. Systemic mRNA delivery to the lungs by functional polyester-based carriers. *Biomacromolecules* **18**, 4307–4315 (2017).
25. Kazi, D. S. et al. Cost-effectiveness of PCSK9 inhibitor therapy in patients with heterozygous familial hypercholesterolemia or atherosclerotic cardiovascular disease. *JAMA* **316**, 743–753 (2016).
26. Wittrup, A. et al. Visualizing lipid-formulated siRNA release from endosomes and target gene knockdown. *Nat. Biotechnol.* **33**, 870–976 (2015).
27. Cheng, Q. et al. Dendrimer-based lipid nanoparticles deliver therapeutic FAH mRNA to normalize liver function and extend survival in a mouse model of hepatorenal tyrosinemia type I. *Adv. Mater.* **30**, e1805308 (2018).
28. Zhou, K. et al. Modular degradable dendrimers enable small RNAs to extend survival in an aggressive liver cancer model. *Proc. Natl Acad. Sci. USA* **113**, 520–525 (2016).
29. Zhang, S. et al. Knockdown of anillin actin binding protein blocks cytokinesis in hepatocytes and reduces liver tumor development in mice without affecting regeneration. *Gastroenterology* **154**, 1421–1434 (2018).
30. Zhang, S. et al. The polyploid state plays a tumor suppressive role in the liver. *Dev. Cell* **44**, 447–459 (2018).
31. Akinc, A. et al. The Onpattro story and the clinical translation of nanomedicines containing nucleic acid-based drugs. *Nat. Nanotechnol.* **14**, 1084–1087 (2019).
32. Sabnis, S. et al. A novel amino lipid series for mRNA delivery: improved endosomal escape and sustained pharmacology and safety in non-human primates. *Mol. Ther.* **26**, 1509–1519 (2018).
33. Hassett, K. J. et al. Optimization of lipid nanoparticles for intramuscular administration of mRNA vaccines. *Mol. Ther. - Nucl. Acids* **15**, 1–11 (2019).
34. Ramaswamy, S. et al. Systemic delivery of factor IX messenger RNA for protein replacement therapy. *Proc. Natl Acad. Sci. USA* **114**, E1941–E1950 (2017).
35. Love, K. et al. Lipid-like materials for low-dose, in vivo gene silencing. *Proc. Natl Acad. Sci. USA* **107**, 1864–1869 (2010).
36. Kauffman, K. J. et al. Optimization of lipid nanoparticle formulations for mRNA delivery in vivo with fractional factorial and definitive screening designs. *Nano Lett.* **15**, 7300–7306 (2015).
37. Hendel, A. et al. Chemically modified guide RNAs enhance CRISPR–Cas genome editing in human primary cells. *Nat. Biotechnol.* **33**, 985–989 (2015).
38. Yin, H. et al. Therapeutic genome editing by combined viral and non-viral delivery of CRISPR system components in vivo. *Nat. Biotechnol.* **34**, 328–333 (2016).
39. Yin, H. et al. Structure-guided chemical modification of guide RNA enables potent non-viral in vivo genome editing. *Nat. Biotechnol.* **35**, 1179 (2017).
40. Wang, L. et al. Meganuclease targeting of PCSK9 in macaque liver leads to stable reduction in serum cholesterol. *Nat. Biotechnol.* **36**, 717–725 (2018).
41. Amoasii, L. et al. Gene editing restores dystrophin expression in a canine model of Duchenne muscular dystrophy. *Science* **362**, 86–91 (2018).
42. Zuris, J. A. et al. Cationic lipid-mediated delivery of proteins enables efficient protein-based genome editing in vitro and in vivo. *Nat. Biotechnol.* **33**, 73–80 (2015).
43. Sun, W. J. et al. Self-assembled DNA nanoclews for the efficient delivery of CRISPR-Cas9 for genome editing. *Angew. Chem. Int. Ed.* **54**, 12029–12033 (2015).
44. Staahl, B. T. et al. Efficient genome editing in the mouse brain by local delivery of engineered Cas9 ribonucleoprotein complexes. *Nat. Biotechnol.* **35**, 431–434 (2017).
45. Finn, J. D. et al. A single administration of CRISPR/Cas9 lipid nanoparticles achieves robust and persistent in vivo genome editing. *Cell Rep.* **22**, 2227–2235 (2018).
46. Tabebordbar, M. et al. In vivo gene editing in dystrophic mouse muscle and muscle stem cells. *Science* **351**, 407–411 (2016).
47. Kamath, A. T. et al. The development, maturation, and turnover rate of mouse spleen dendritic cell populations. *J. Immunol.* **165**, 6762–6770 (2000).
48. Xue, W. et al. CRISPR-mediated direct mutation of cancer genes in the mouse liver. *Nature* **514**, 380–384 (2014).
49. Monopoli, M. P., Aberg, C., Salvati, A. & Dawson, K. A. Biomolecular coronas provide the biological identity of nanosized materials. *Nat. Nanotechnol.* **7**, 779–786 (2012).
50. Akinc, A. et al. Targeted delivery of RNAi therapeutics with endogenous and exogenous ligand-based mechanisms. *Mol. Ther.* **18**, 1357–1364 (2010).

Methods

Materials. 5A2-SC8 (ref. [28]) and C12-200 (ref. [35]) were synthesized and purified by following published protocols. DLin-MC3-DMA[11] was purchased from MedKoo Biosciences. DOTAP, DDAB, EPC, 18PA (sodium salt), 14PA (sodium salt), 18BMP (ammonium salt) (18/1 Hemi BMP), DODAP, DSPC, DOCPe and DOPE were purchased from Avanti Polar Lipids. Cholesterol was purchased from Sigma. DMG-PEG (MW 2000) (DMG-PEG2000) was purchased from NOF America Corporation. Cas9 protein was purchased from Thermo Fisher. Sodium dodecyl sulfate was purchased from Sigma. The ONE-Glo + Tox Luciferase Reporter assay kit was purchased from Promega Corporation. Pur-A-Lyzer Midi Dialysis Kits (WMCO, 3.5 kDa) were purchased from Sigma. The 4',6-diamidino-2-phenylindole dihydrochloride (DAPI) was purchased from Thermo Fisher. Cas9 mRNA was produced using in vitro translation (IVT). Luc mRNA and mCherry mRNA were purchased from TriLink BioTechnologies. D-Luciferin (sodium salt) was purchased from Gold Biotechnology. Modified sgTom1, sgPTEN and sgPCSK9 (Supplementary Table 2) were purchased from Synthego.

Nanoparticle formation. RNA-loaded LNP formulations were formed using the ethanol dilution method[28]. The liver-targeted mRNA formulation (mDLNP) was developed and reported in our previous paper[27], and the base formulations were prepared as previously described[11,35]. Unless otherwise stated, all lipids with specified molar ratios were dissolved in ethanol and RNA was dissolved in 10 mM citrate buffer (pH 4.0). The two solutions were rapidly mixed at an aqueous to ethanol ratio of 3/1 by volume (3/1, aq./ethanol, vol./vol.) to satisfy a final weight ratio of 40/1 (total lipids/mRNA), then incubated for 10 min at room temperature. To prepare SORT LNP formulations containing anionic SORT lipids (such as 18PA, 14PA and 18BMP), the anionic lipids were first dissolved in tetrahydrofuran then mixed with other lipid components in ethanol, yielding formulations with mRNA buffer (10 mM, pH 3.0) as described above. All formulations were named based on the additional lipids. Taking DOTAP mDLNP as an example, the internal molar ratio of mDLNP was fixed as reported in our previous paper with a 5A2-SC8/DOPE/cholesterol/DMG-PEG ratio of 15/15/30/3 (ref. [27]). DOTAP, used as the additional lipid, was dissolved into the above ethanol lipid mixture in a specified amount, making the molar ratio of 5A2-SC8/DOPE/cholesterol/DMG-PEG/DOTAP equal to 15/15/30/3/*X*, where the *X* represents the molar ratio of DOTAP lipid, then rapidly mixed with aq. mRNA solutions following the above standard protocol, producing SORT LNPs named *Y*% DOTAP, where *Y* is the molar per cent of DOTAP as a proportion of the total lipids. Formulations with other additional lipids were prepared in a manner similar to the above methods (Supplementary Fig. 1 and Supplementary Table 1). As a representative example, liver-targeted SORT LNPs (20% DODAP) were prepared as follows. A solution of lipids in ethanol was prepared consisting of 7.59 mM 5A2-SC8, 7.59 mM DOPE, 15.18 mM cholesterol, 1.52 mM DMG-PEG2000 and 7.97 mM DODAP to make the final molar ratio of 19.05/19.05/38.1/3.81/20. To reach a final ratio of 40/1 (wt/wt) of total lipids/total RNAs, 1.16 µl lipid solution was used per µg of RNA. For example, to make a final 5-µg RNA formulation, a mixture of 5.8 µl of lipid and 9.2 µl of ethanol were mixed (total 15 µl), and then a 45 µl mRNA solution was prepared consisting of 5 µg of RNA in citrate buffer (10 mM, pH 4.0). Then 45 µl of the mRNA solution was rapidly combined with 15 µl of the ethanol/lipid solution to form 20% DODAP SORT LNPs. For Cas9/sgRNA RNP encapsulation, 1× PBS buffer was used for formulation and the molar ratio of Cas9 and sgRNA was fixed at 1/3. After SORT LNP formation, the fresh LNP formulations were diluted with 1× PBS to 0.5 ng µl^{-1} mRNA (with a final ethanol concentration < 5%) for in vitro assays and size detection using dynamic light scattering (Malvern MicroV model; He–Ne laser, wavelength = 632 nm). For in vivo experiments, the formulations were dialysed (Pur-A-Lyzer Midi Dialysis Kits, WMCO 3.5 kDa) against 1× PBS for 2 h, and diluted with PBS to 15 µl g^{-1} for i.v. injections.

In vivo Luc mRNA delivery. C57BL/6 mice with weights of 18–20 g were i.v. injected with various Luc mRNA formulations: $n = 3$–4 per group. At the stated detection timepoints, mice were injected with D-Luciferin (150 mg kg^{-1}, intraperitoneal) and imaged using an IVIS Lumina system (Perkin Elmer). In this work, bioluminescence imaging was performed at various timepoints (3, 6, 8 and 24 h) following injection of various Luc mRNA doses (0.02 to 0.5 mg kg^{-1}, i.v.). To further quantify Luc mRNA delivery in vivo, we normalized the relative luciferase expression per milligram of tissue and per microgram of total protein. Briefly, LNPs were formed as described above and mice were i.v. injected with a dose of 0.1 mg kg^{-1} Luc mRNA. After 6 h, tissues were collected and cut using scissors, and then a known weight of tissue (20–30 mg) was homogenized using T-PER tissue protein extraction reagent (Thermo Fisher). Then 20 µl of supernatant was used to measure the luciferase expression using ONE-Glo kits based on Promega's standard protocol, and 10 µl of supernatant was used to measure the total protein using a bicinchoninic acid kit (Thermo Fisher). Finally, relative luciferase expression was normalized against tissue weight and total protein.

LNP stability testing. To study LNP stability, the sizes, polydispersity index and encapsulation efficacy were monitored for 1 week during storage in PBS at 4 °C. mDLNPs, 50% DOTAP SORT LNPs (lung), 30% 18PA SORT LNPs (spleen) and 20% DODAP SORT LNPs (liver) were formed as described above and dialysed with 1× PBS, and then diluted to 5 ng µl^{-1} Luc mRNA in 1× PBS ($n = 3$). Then 250 µl was pipetted into DLS ultramicro cuvettes for size and polydispersity index monitoring and 250 µl was pipetted into a 1.5-ml tube for encapsulation efficacy evaluation using the Ribogreen assay for 1 week. Additionally, to evaluate mRNA delivery efficacy in vivo, mice were i.v. injected with LNPs that had been stored for 1 week at 4 °C, and the luminescence was measured 6 h after injection.

mRNA synthesis. Optimized IL-10, hEPO, mKL ECD, Cre recombinase and Cas9 mRNAs were produced using IVT. Briefly, the coding fragments of each protein were prepared using a PCR programme (Supplementary Table 3). Then, these fragments were cloned into pCS2+MT vectors with optimized 5'(3')-untranslated regions and poly A sequences. IVT reactions were performed following standard protocols but with N1-methylpseudouridine-5'-triphosphate replacing the typical uridine triphosphate. Finally, the mRNA was capped (Cap-1) using the vaccinia capping enzyme and 2'-*O*-methyltransferase New England Biolabs (NEB). The coding sequences for these proteins are detailed in the Supplementary Information.

Western blot. The quality of IVT Cas9 mRNA was analysed using a western blot. The day before transfection, 293 T cells were seeded into a 12-well plate with a density of 1×10^5 cells per well. The cells were treated with various formulations in a total volume of 600 µl for another 24 h, including mCherry mDLNP (0.5 µg of mRNA per well), mCherry mDLNP (1.0 µg of mRNA per well), IVT Cas9 mDLNP (0.5 µg of mRNA per well), IVT Cas9 mDLNP (1.0 µg of mRNA per well) and Lipofectamine2000/Cas9 plasmid DNA (0.5 µg of plasmid DNA per well). After washing three times with 1× PBS, 100 µl of lysis buffer (50 mM Tris–HCl, pH 7.4, with 150 mM NaCl, 1 mM EDTA and 1% Triton X-100) and 1 µl of protein inhibitor cocktail (100×, Thermo Fisher) were added into each well and rocked for 20 min at room temperature. Cell lysates were collected in 1.6-ml tubes and centrifuged for 10 min (13,000*g*) at 4 °C. The supernatants were collected in new tubes and stored at −80 °C if not used immediately. Before executing a western blot, the protein concentrations were measured using a BCA assay kit (Thermo Fisher). Then 15 µg of total proteins was loaded and separated using a 4–20% polyacrylamide gel (Thermo Fisher). The separated proteins were then transferred onto a poly(vinylidene) membrane (BioRad) and blocked with 5% BSA (dissolved in PBST, Thermo Fisher) for 1 h at room temperature. Primary antibodies were applied overnight at 4 °C. After washing four times using PBST, the membrane was incubated using a secondary antibody for 1 h at room temperature then imaged with an ECL substrate after washing four times with PBST. For PCSK9 detection in liver tissue, the total protein was extracted using RIPA lysis and extraction buffer (Thermo Fisher) using standard protocols, and then a western blot was executed as described above.

In vivo toxicity evaluation. Male C57BL/6 mice, with weights of 18–20 g, were randomly divided into five groups: $n = 4$ per group. To give maximum toxicity exposure in vivo, we selected a high dose of mRNA (1 mg kg^{-1} mCherry mRNA) for i.v. injection, and three tissue-targeting formulations were used: 50% DOTAP SORT LNPs for lung; 30% 18PA SORT LNPs for spleen; and 20% DODAP SORT LNPs for liver. Lipopolysaccharide (5 mg kg^{-1}) was intraperitoneal injected as the positive control and PBS was i.v. injected as the negative control. After 24 and 48 h, whole blood was collected and the serum was separated. Next, the liver function (AST and ALT) and renal function (BUN and CREA) was measured using the UT Southwestern Metabolic Phenotyping Core, and tissue (heart, liver, spleen, lung and kidney) sections with H&E staining were analysed at the UT Southwestern Tissue Management shared resource. To further study the potential toxicity in vivo, we performed two i.v. injections with doses of 1 mg kg^{-1} mCherry mRNA. Briefly, the mice were injected with SORT LNPs at day 0 and day 3, and the serum was separated at 24 and 48 h after the second injection, and then the liver function and renal function were measured as described above. In addition, the serum cytokines (IL-1β and TNF-α) were measured at the UT Southwestern Genomics Sequencing & Microarray Core facility.

In vivo therapeutic mRNA delivery. Male C57BL/6 mice, with weights of 18–20 g, were randomly divided into five groups: $n = 3$ per group. For therapeutic mRNA delivery, we prepared three different mRNAs: IL-10, hEPO and mKL. For IL-10 and hEPO mRNA delivery, we applied different doses to target all three organs, lung (50% DOTAP SORT LNPs), spleen (30% 18PA SORT LNPs) and liver (20% DODAP SORT LNPs). At the same time, we included Onpattro (DLin-MC3-DMA LNPs)[31] for efficacy comparison of the liver-targeted formulations. At 6 h after i.v. injection, the serum was separated from the whole blood, and the concentrations were detected using enzyme-linked immunosorbent assay (ELISA) kits (IL-10 Mouse ELISA Kit and Erythropoietin Human ELISA Kit, Thermo Fisher). Furthermore, we evaluated the hEPO protein kinetics in serum with 20% DODAP SORT LNPs (0.3 mg/kg), we collected serum from 0 h to day 7 after i.v. injection, and then quantified the hEPO using an ELISA assay. For the mKL assay, quantification of serum was analysed at the UT Southwestern Physiology Core facility (O'Brien Kidney Center).

Gene editing (Cre mRNA) in the tdTom mice model. Cre mRNA formulations were prepared as described above and i.v. injections were performed (0.3 mg kg^{-1}

Cre mRNA). After 2 d, mice ($n = 3$ per group) were killed and the major organs were imaged using an IVIS Lumina system (Perkin Elmer).

Cell isolation and staining for flow cytometry. To test the tdTom$^+$ cells in the different cell types of each organ, cell isolation and staining was performed after 2 d of treatment with Cre mRNA formulations (0.3 mg kg^{-1}), followed by flow cytometry analysis.

For hepatocyte isolation, a two-step collagenase perfusion was executed as described previously[27]. Briefly, mice were anesthetized using isofluorane then fixed. Perfusion, initially using liver perfusion medium (Thermo Fisher, 17701038) for 7–10 min, then switching to liver digestion medium (Thermo Fisher, 17703034) for another 7–10 min, was performed. The liver was collected on a plate containing 10 ml of liver digestion medium and cut to release the hepatocytes. The released hepatocytes were then collected and washed with ice-cold hepatocyte wash medium (Thermo Fisher, 17704024) via low speed centrifugation (50*g*) for 5 min. The supernatant was decanted and the pellet was resuspended with an ice-cold hepatocyte wash medium. The cell suspension was passed through a 100 µM filter into a new tube. The hepatocyte–cell suspension was washed twice with ice-cold hepatocyte wash medium and and once with 1× PBS via centrifugation (50*g*) for 5 min. Afterwards, the hepatocytes were isolated further by straining through a 100-µm filter and using low speed (50*g*) centrifugation for 5 min, the supernatant was then removed and the resuspended hepatocytes were analysed using a fluorescence-activated cell sorting (FACS) Aria II SORP machine (BD Biosciences).

For isolation and staining of spleen cells, the removed spleen was minced using a sterile blade and homogenized in 250 µl of 1× digestion medium (45 units µl^{-1} collagenase I, 25 units µl^{-1} DNase I and 30 units µl^{-1} hyaluronidase). The spleen solution was transferred into a 15-ml tube that contained 5–10 ml of 1× digestion medium. Next, the spleen solution was filtered using a 70-µm filter and washed once with 1× PBS. A cell pellet was obtained by centrifuging for 5 min at a speed of 300*g* at 4 °C. The supernatant was removed and the cell pellet was resuspended in 2 ml of 1× red blood cell lysis buffer (BioLegend, 420301) and incubated on ice for 5 min. After incubation, 4 ml of cell staining buffer (BioLegend) was added to stop red blood cell lysis. The solution was centrifuged again at 300*g* for 5 min to obtain a cell pellet. The single cells were resuspended in cell staining buffer and added to flow tubes that contained antibodies (total volume 100 µl). The cells were incubated with antibodies for 20 min in the dark at 4 °C. The stained cells were washed twice with 1 mL 1X PBS, then resuspended in 500 µL 1X PBS for flow cytometry analysis. The antibodies used were, Pacific Blue anti-mouse CD45 (BioLegend, 103126), Alexa Fluor 488 anti-mouse/human CD11b (BioLegend, 101217), Alexa Fluor 647 anti-mouse CD19 (BioLegend, 115522) and PerCP-Cyanine5.5 anti-mouse CD3e (145-2C11) (Tonbo Biosciences, 65-0031). Ghost Dye Red 780 (Tonbo Biosciences, 13-0865-T500) was used to discriminate live cells. The spleen cells were analysed using a LSRForessa SORP machine (BD Biosciences).

For isolation and staining of lung cells, isolated lungs were minced using a sterile blade and then transferred into a 15-ml tube that contained 10 ml of 2× digestion medium (90 units µl^{-1} collagenase I, 50 units µl^{-1} DNase I and 60 units µl^{-1} hyaluronidase) and incubated at 37 °C for 1 h with shaking. After incubation, any remaining lung tissue was homogenized. The following steps were similar to the spleen protocol described above. The antibodies used here were Pacific Blue anti-mouse CD45, Alexa Fluor 488 anti-mouse CD31 (BioLegend, 102414) and Alexa Fluor 647 anti-mouse CD326 (Ep-CAM) (BioLegend, 118212). Ghost Dye Red 780 was used to discriminate live cells. The lung cells were analysed using a LSRForessa SORP machine.

Gene editing (Cas9 mRNA/sgRNA and Cas9/sgRNA RNPs) in the tdTom mice model. To evaluate in vivo gene editing, tdTom mice with comparable weights and of the same sex were selected. We co-delivered Cas9 mRNA and sgRNA (Supplementary Table 2) to tdTom mice. Cas9 mRNA/sgTom1 (4/1, wt/wt) was co-delivered using various formulations and with the total RNA dose equal to 2.5 mg kg^{-1}. Ten days following i.v. injection, the main organs were removed and imaged on an IVIS Lumina system. For spleen-targeted formulations, the total RNA dose was 4 mg kg^{-1} and a weight ratio of Cas9 mRNA to sgTom1 was 2/1, with a detection time of 2 d. For RNP delivery, the molar ratio of Cas9 protein to sgRNA was fixed at 1/3, the injection dose was 1.5 mg kg^{-1} RNA, and the detection time was 7 d after injection ($n = 3$ per group). To confirm tdTom expression, tissue sections were prepared and imaged using confocal microscopy (Zeiss LSM 700). Briefly, tissue blocks were embedded into optimal cutting temperature compounds (Sakura Finetek) and co-sectioned (8 µm) on a Cryostat instrument (Leica Biosystems). The mounted tissue slices were stained with DAPI (Vector Laboratories) before confocal microscopy imaging.

Gene editing (Cas9 mRNA/sgPTEN and Cas9/sgRNA RNPs) in C57BL/6 mice. To examine endogenous gene editing in vivo, PTEN was selected. Wild-type C57BL/6 mice were i.v. injected with various carriers for co-delivery of Cas9 mRNA and modified sgPTEN (Supplementary Table 2) at a total dose of 2.5 mg kg^{-1} (4/1, mRNA/sgRNA, wt/wt) ($n = 3$ per group). After 10 d, the tissue was collected and the genomic DNA extracted using a PureLink Genomic DNA Mini Kit (Thermo Fisher). For spleen-targeted formulations, the total RNA dose was 4 mg kg^{-1}, the Cas9 mRNA/sgTom1 ratio was 2/1 (wt/wt) and the detection time was 2 d after injection. For RNP delivery, the molar ratio of Cas9 protein to sgRNA was fixed at 1/3, the injection dose was 1.5 mg kg^{-1} RNA and the detection time was 7 d after injection ($n = 3$ per group). After obtaining the PTEN PCR products, a T7E1 assay[51,52] was performed to confirm gene editing efficacy using the established manufacturer protocol (NEB) (Supplementary Table 3); detailed instructions including an interactive protocol are available online (https://www.neb.com/protocols/2014/08/11/determining-genome-targeting-efficiency-using-t7-endonuclease-i). The evaluation of PTEN editing was executed on H&E and IHC-stained tissue sections. Briefly, paraformaldehyde fixed tissues were embedded in paraffin, sectioned and H&E stained at the UT Southwestern Molecular Pathology Core facility. The 4-µm sections were analysed in the standard fashion for IHC and detection was performed using an Elite ABC Kit and DAB Substrate (Vector Laboratories). For off-target prediction of sgPTEN, the Cas-OFFinder webtool was employed (http://www.rgenome.net/cas-offinder/). Eight potential targeted positions were amplified using a PCR reaction, and then analysed using a T7E1 assay and Sanger sequencing.

Gene editing (Cas9 mRNA/sgPCSK9) in C57BL/6 mice. To perform liver PCSK9 gene knockout in vivo, wild-type C57BL/6 mice were i.v. injected three times (day 0, day 2 and day 4) for co-delivery of Cas9 mRNA and modified sgPCSK9 (Supplementary Table 2) at a total dose of 2.5 mg kg^{-1} (1/1, mRNA/sgRNA, wt/wt) ($n = 4$ per group). After 7 and 9 d, whole blood was collected and the serum was separated for serum PCSK9 protein detection using an ELISA assay kit (Abcam). Detection of PCSK9 protein expression in liver tissue was detected using western blot (day 9). For gene knockout validation at the genomic level, liver tissue was collected at day 9 and the genomic DNA was extracted using a PureLink Genomic DNA Mini Kit (Thermo Fisher). After examining the PCSK9 PCR process, the indel of PCSK9 was analysed using a T7E1 assay (described above) and the TIDE webtool (https://tide.deskgen.com/) (Supplementary Table 3).

Display items. The images of mice and syringes (Figs. 1a,2d,3a and 4a,h, and Supplementary Figs. 5–8, 13, 22 and 25) and organs (Figs. 1a and 2a–c, and Supplementary Figs. 9 and 10) were created with BioRender.com.

Reporting Summary. Further information on research design is available in the Nature Research Reporting Summary linked to this article.

Data availability

The data that support the plots within this paper and other findings of this study are available from the corresponding author upon reasonable request.

References

51. Liu, J. J. et al. CasX enzymes comprise a distinct family of RNA-guided genome editors. *Nature* **566**, 218–223 (2019).
52. Nihongaki, Y., Kawano, F., Nakajima, T. & Sato, M. Photoactivatable CRISPR–Cas9 for optogenetic genome editing. *Nat. Biotechnol.* **33**, 755–760 (2015).

Acknowledgements

D.J.S. acknowledges financial support from the National Institutes of Health (NIH) National Institute of Biomedical Imaging and Bioengineering (NIBIB) (grant no. R01 EB025192-01A1), the Cystic Fibrosis Foundation (CFF) (grant no. SIEGWA18XX0), the American Cancer Society (ACS) (grant no. RSG-17-012-01) and the Welch Foundation (grant no. I-1855). We acknowledge the UTSW Tissue Resource, supported in part by the National Cancer Institute (grant no. 5P30CA142543), the Moody Foundation Flow Cytometry Facility and the UTSW Proteomics Core. We thank Y. Jia, Y.-H. Lin, Y. Wei and H. Zhu for assistance with tissue processing and analyses.

Author contributions

Q.C., T.W. and D.J.S. conceived and designed the experiments and wrote the manuscript. Q.C., T.W., L.F., L.T.J. and S.A.D. performed experiments. All authors discussed the results and commented on the manuscript. D.J.S. directed the research.

Competing interests

D.J.S., Q.C., T.W. and the Reagents of the University of Texas System have filed patent applications on SORT and related technologies. D.J.S. is a co-founder of ReCode Therapeutics, which has licensed intellectual property from UT Southwestern.

Additional information

Supplementary information is available for this paper at https://doi.org/10.1038/s41565-020-0669-6.

Correspondence and requests for materials should be addressed to D.J.S.

Peer review information *Nature Nanotechnology* thanks Roy van der Meel and the other, anonymous, reviewer(s) for their contribution to the peer review of this work.
Reprints and permissions information is available at www.nature.com/reprints.

nature research

Corresponding author(s): Daniel J. Siegwart (NNANO-19112620B)

Last updated by author(s): Jan 30, 2020

Reporting Summary

Nature Research wishes to improve the reproducibility of the work that we publish. This form provides structure for consistency and transparency in reporting. For further information on Nature Research policies, see Authors & Referees and the Editorial Policy Checklist.

Statistics

For all statistical analyses, confirm that the following items are present in the figure legend, table legend, main text, or Methods section.

n/a	Confirmed
☐	☒ The exact sample size (*n*) for each experimental group/condition, given as a discrete number and unit of measurement
☐	☒ A statement on whether measurements were taken from distinct samples or whether the same sample was measured repeatedly
☐	☒ The statistical test(s) used AND whether they are one- or two-sided *Only common tests should be described solely by name; describe more complex techniques in the Methods section.*
☒	☐ A description of all covariates tested
☒	☐ A description of any assumptions or corrections, such as tests of normality and adjustment for multiple comparisons
☐	☒ A full description of the statistical parameters including central tendency (e.g. means) or other basic estimates (e.g. regression coefficient) AND variation (e.g. standard deviation) or associated estimates of uncertainty (e.g. confidence intervals)
☐	☒ For null hypothesis testing, the test statistic (e.g. *F*, *t*, *r*) with confidence intervals, effect sizes, degrees of freedom and *P* value noted *Give P values as exact values whenever suitable.*
☒	☐ For Bayesian analysis, information on the choice of priors and Markov chain Monte Carlo settings
☒	☐ For hierarchical and complex designs, identification of the appropriate level for tests and full reporting of outcomes
☒	☐ Estimates of effect sizes (e.g. Cohen's *d*, Pearson's *r*), indicating how they were calculated

Our web collection on statistics for biologists contains articles on many of the points above.

Software and code

Policy information about availability of computer code

Data collection	Zetasizer software version 7.13 (Malvern Panalytical) ZEN x64 software version 1.1.0 (Carl Zeiss Microscopy GmbH) Living Image software version 4.3 (64-bit, Caliper Life Sciences) BD FACSDiva software version 8.0.1 (BD LSRFortessa)
Data analysis	FLOWJO software version 7.6 (FLOWJO) ZEN 2010 software version 6.0.62 (Carl Zeiss MicroImaging GmbH) GraphPad Prism 7 software version 7.04 (GraphPad Software) Living Image software version 4.3 (64-bit, Caliper Life Sciences) TIDE Analysis tool (no version information available), (analyzing indels by decomposition): https://tide.deskgen.com/

For manuscripts utilizing custom algorithms or software that are central to the research but not yet described in published literature, software must be made available to editors/reviewers. We strongly encourage code deposition in a community repository (e.g. GitHub). See the Nature Research guidelines for submitting code & software for further information.

Data

Policy information about availability of data

All manuscripts must include a data availability statement. This statement should provide the following information, where applicable:

- Accession codes, unique identifiers, or web links for publicly available datasets
- A list of figures that have associated raw data
- A description of any restrictions on data availability

The authors declare that all data supporting the findings of this study are available within the paper [and its supplementary information files].
The data that support the findings of this study are available from the corresponding author upon reasonable request.

Field-specific reporting

Please select the one below that is the best fit for your research. If you are not sure, read the appropriate sections before making your selection.

☒ Life sciences ☐ Behavioural & social sciences ☐ Ecological, evolutionary & environmental sciences

For a reference copy of the document with all sections, see nature.com/documents/nr-reporting-summary-flat.pdf

Life sciences study design

All studies must disclose on these points even when the disclosure is negative.

Sample size	Power analysis was employed to determine sample sizes.
Data exclusions	No data were excluded.
Replication	We confirm that all attempts at replication were successful. We have used C57BL/6 mice and tdTomato reporter mice (Ai9 mice) mice to confirm tissue specific mRNA delivery and gene editing in lung, spleen, and liver. The narrow variations also confirmed that our experimental findings are reproducible. Key data generated by one co-author were repeated by other co-authors.
Randomization	For animal experiments, mice with ages of 8-10 weeks were randomly allocated into each treatment group.
Blinding	Due to the proof-of-concept developmental nature of this study, true blinding of experiments was not performed. However, data collection and analyses for some experiments were performed by separate individuals. In some cases, these collectors/analyzers were not aware which samples corresponded to which experimental groups at the time of data collection and analysis.

Behavioural & social sciences study design

All studies must disclose on these points even when the disclosure is negative.

Study description	*Briefly describe the study type including whether data are quantitative, qualitative, or mixed-methods (e.g. qualitative cross-sectional, quantitative experimental, mixed-methods case study).*
Research sample	*State the research sample (e.g. Harvard university undergraduates, villagers in rural India) and provide relevant demographic information (e.g. age, sex) and indicate whether the sample is representative. Provide a rationale for the study sample chosen. For studies involving existing datasets, please describe the dataset and source.*
Sampling strategy	*Describe the sampling procedure (e.g. random, snowball, stratified, convenience). Describe the statistical methods that were used to predetermine sample size OR if no sample-size calculation was performed, describe how sample sizes were chosen and provide a rationale for why these sample sizes are sufficient. For qualitative data, please indicate whether data saturation was considered, and what criteria were used to decide that no further sampling was needed.*
Data collection	*Provide details about the data collection procedure, including the instruments or devices used to record the data (e.g. pen and paper, computer, eye tracker, video or audio equipment) whether anyone was present besides the participant(s) and the researcher, and whether the researcher was blind to experimental condition and/or the study hypothesis during data collection.*
Timing	*Indicate the start and stop dates of data collection. If there is a gap between collection periods, state the dates for each sample cohort.*
Data exclusions	*If no data were excluded from the analyses, state so OR if data were excluded, provide the exact number of exclusions and the rationale behind them, indicating whether exclusion criteria were pre-established.*
Non-participation	*State how many participants dropped out/declined participation and the reason(s) given OR provide response rate OR state that no participants dropped out/declined participation.*
Randomization	*If participants were not allocated into experimental groups, state so OR describe how participants were allocated to groups, and if allocation was not random, describe how covariates were controlled.*

Ecological, evolutionary & environmental sciences study design

All studies must disclose on these points even when the disclosure is negative.

Study description	*Briefly describe the study. For quantitative data include treatment factors and interactions, design structure (e.g. factorial, nested, hierarchical), nature and number of experimental units and replicates.*
Research sample	*Describe the research sample (e.g. a group of tagged Passer domesticus, all Stenocereus thurberi within Organ Pipe Cactus National Monument), and provide a rationale for the sample choice. When relevant, describe the organism taxa, source, sex, age range and*

any manipulations. State what population the sample is meant to represent when applicable. For studies involving existing datasets, describe the data and its source.

Sampling strategy	Note the sampling procedure. Describe the statistical methods that were used to predetermine sample size OR if no sample-size calculation was performed, describe how sample sizes were chosen and provide a rationale for why these sample sizes are sufficient.
Data collection	Describe the data collection procedure, including who recorded the data and how.
Timing and spatial scale	Indicate the start and stop dates of data collection, noting the frequency and periodicity of sampling and providing a rationale for these choices. If there is a gap between collection periods, state the dates for each sample cohort. Specify the spatial scale from which the data are taken
Data exclusions	If no data were excluded from the analyses, state so OR if data were excluded, describe the exclusions and the rationale behind them, indicating whether exclusion criteria were pre-established.
Reproducibility	Describe the measures taken to verify the reproducibility of experimental findings. For each experiment, note whether any attempts to repeat the experiment failed OR state that all attempts to repeat the experiment were successful.
Randomization	Describe how samples/organisms/participants were allocated into groups. If allocation was not random, describe how covariates were controlled. If this is not relevant to your study, explain why.
Blinding	Describe the extent of blinding used during data acquisition and analysis. If blinding was not possible, describe why OR explain why blinding was not relevant to your study.

Did the study involve field work? ☐ Yes ☐ No

Field work, collection and transport

Field conditions	Describe the study conditions for field work, providing relevant parameters (e.g. temperature, rainfall).
Location	State the location of the sampling or experiment, providing relevant parameters (e.g. latitude and longitude, elevation, water depth).
Access and import/export	Describe the efforts you have made to access habitats and to collect and import/export your samples in a responsible manner and in compliance with local, national and international laws, noting any permits that were obtained (give the name of the issuing authority, the date of issue, and any identifying information).
Disturbance	Describe any disturbance caused by the study and how it was minimized.

Reporting for specific materials, systems and methods

We require information from authors about some types of materials, experimental systems and methods used in many studies. Here, indicate whether each material, system or method listed is relevant to your study. If you are not sure if a list item applies to your research, read the appropriate section before selecting a response.

Materials & experimental systems

n/a	Involved in the study
☐	☒ Antibodies
☐	☒ Eukaryotic cell lines
☒	☐ Palaeontology
☐	☒ Animals and other organisms
☒	☐ Human research participants
☒	☐ Clinical data

Methods

n/a	Involved in the study
☒	☐ ChIP-seq
☐	☒ Flow cytometry
☒	☐ MRI-based neuroimaging

Antibodies

Antibodies used	1. We used multiple monoclonal antibodies in the flow cytometry to determine tissue specific editing by Cre mRNA in tdTomato mice in Figure 3 and SI figures. These antibodies are: Pacific Blue anti-mouse CD45 (BioLegend, 103126), Alexa Fluor 488 anti-mouse/human CD11b (BioLegend, 101217), Alexa Fluor 647 anti-mouse CD19 (BioLegend, 115522), PerCP-Cyanine5.5 Anti-Mouse CD3e (145-2C11) (Tonbo Biosciences, 65-0031), Alexa Fluor 488 anti-mouse CD31 (BioLegend, 102414) and Alexa Fluor 647 anti-mouse CD326 (Ep-CAM) (BioLegend, 118212). 2. We used Cas9 monoclonal antibody in the western blot to determine Cas9 mRNA expression in cells in Figure S19. This antibody is Cas9 (7A9-3A3)(Cell Signaling Technology, 14697). 3. We used PTEN monoclonal antibody in the IHC to determine PTEN editing in Figure 4. This antibody is PTEN (138G6) Rabbit mAb (Cell Signaling Technology, 9559). 4. We used PCSK9 monoclonal antibody in the western blot to determine PCSK9 knockout in Figure 4. This antibody is Recombinant Anti-PCSK9 antibody [EPR17827-117] (Abcam, ab185194).

Validation

1. The Pacific Blue anti-mouse CD45 has been validated to be used for immunofluorescent staining with flow cytometric analysis. The suggested use of this reagent is ≤ 0.25 µg per million cells in 100 µl volume from the manufacturer's website and it is also mentioned species reactivity with mouse thymus or spleen. (https://www.biolegend.com/en-us/products/pacific-blue-anti-mouse-cd45-antibody-3102). After titration, we finally used 1/400 dilution for lung cell types and 1/200 dilution for spleen.
2. Alexa Fluor 488 anti-mouse/human CD11b has been validated to be used for immunofluorescent staining with flow cytometric analysis. The suggested use of this reagent is ≤ 0.25 µg per million cells in 100 µl volume from the manufacturer's website and it is also mentioned species reactivity with C57BL/10 splenocytes.(https://www.biolegend.com/en-us/products/alexa-fluor-488-anti-mouse-human-cd11b-antibody-2700). After titration, we finally used 1/1600 dilution for analysis.
3. Alexa Fluor 647 anti-mouse CD19 has been validated to be used for immunofluorescent staining with flow cytometric analysis. The suggested use of this reagent is ≤ 0.25 µg per million cells in 100 µl volume from the manufacturer's website and it is also mentioned species reactivity with Mouse CD19-expressing K562 human erythroleukemia cells. (https://www.biolegend.com/en-us/products/alexa-fluor-647-anti-mouse-cd19-antibody-2705). After titration, we finally used 1/400 dilution for analysis.
4. PerCP-Cyanine5.5 Anti-Mouse CD3e (145-2C11), has been validated to be used for immunofluorescent staining with flow cytometric analysis and mentioned species reactivity with mouse. (https://tonbobio.com/products/percp-cyanine5-5-anti-mouse-cd3e-145-2c11). After titration, we finally used 1/40 dilution for analysis.
5. Alexa Fluor 488 anti-mouse CD31 has been validated to be used for immunofluorescent staining with flow cytometric analysis. The suggested use of this reagent is ≤ 0.25 µg per million cells in 100 µl volume from the manufacturer's website and it is also mentioned species reactivity with C3H/HeJ mouse hematopoietic progenitor cell line 3. (https://www.biolegend.com/en-us/products/alexa-fluor-488-anti-mouse-cd31-antibody-3091). After titration, we finally used 1/800 dilution for analysis.
6. Alexa Fluor 647 anti-mouse CD326 (Ep-CAM) has been validated to be used for immunofluorescent staining with flow cytometric analysis. The suggested use of this reagent is ≤ 0.25 µg per million cells in 100 µl volume from the manufacturer's website and it is also mentioned species reactivity with TE-71 thymic epithelial cell line. (https://www.biolegend.com/en-us/products/alexa-fluor-647-anti-mouse-cd326-ep-cam-antibody-4973). After titration, we finally used 1/1600 dilution for analysis.
7. Cas9 (7A9-3A3) antibody has been validated to be used for western blot at dilution of 1:1000 from the manufacturer's website and it is also mentioned species reactivity with amino terminus of Cas9 from Streptococcus pyogenes. (https://www.cellsignal.com/products/primary-antibodies/cas9-7a9-3a3-mouse-mab/14697)
8. PTEN (138G6) Rabbit mAb antibody has been validated to be used for Immunohistochemistry (Paraffin) at dilution of 1:200 from the manufacturer's website and it is also mentioned species reactivity with human, mouse, rat and monkey. (https://www.cellsignal.com/products/primary-antibodies/pten-138g6-rabbit-mab/9559)
9. Recombinant Anti-PCSK9 antibody [EPR17827-117] antibody has been validated to be used for western blot at dilution of 1:1000 from the manufacturer's website and it is also mentioned species reactivity with mouse. (https://www.abcam.com/pcsk9-antibody-epr17827-117-ab185194.html)

For all antibodies mentioned above, our data provided in the Figures also validated that these primary antibodies can be applied to studies on their purposes.

Eukaryotic cell lines

Policy information about cell lines

Cell line source(s)	Huh7 and A549 cells were originally obtained from ATTC.
Authentication	The cell lines were not further authenticated after receiving from ATTC.
Mycoplasma contamination	The cell lines were not tested for mycoplasma contamination.
Commonly misidentified lines (See ICLAC register)	These cell lines were checked against the ICLAC database. A549 is listed as a possible contaminating cell line.

Palaeontology

Specimen provenance	*Provide provenance information for specimens and describe permits that were obtained for the work (including the name of the issuing authority, the date of issue, and any identifying information).*
Specimen deposition	*Indicate where the specimens have been deposited to permit free access by other researchers.*
Dating methods	*If new dates are provided, describe how they were obtained (e.g. collection, storage, sample pretreatment and measurement), where they were obtained (i.e. lab name), the calibration program and the protocol for quality assurance OR state that no new dates are provided.*

☐ Tick this box to confirm that the raw and calibrated dates are available in the paper or in Supplementary Information.

Animals and other organisms

Policy information about studies involving animals; ARRIVE guidelines recommended for reporting animal research

Laboratory animals	C57BL/6 mice were obtained from the UTSW Mouse Breeding Core Facility. Male and female mice with age of 8-10 weeks were used. B6.Cg-Gt(ROSA)26Sortm9(CAGtdTomato)Hze/J mice (also known as Ai9 or Ai9(RCL-tdT) mice) were obtained from The Jackson Laboratory (007909) and bred to maintain homozygous expression of the Cre reporter allele that has a loxP-flanked STOP cassette preventing transcription of a CAG promoter-driven red fluorescent tdTomato protein. Following Cre-mediated recombination or CRISPR/Cas9 based gene editing, Ai9 mice will express tdTomato fluorescence. Ai9 mice are congenic on the

	C57BL/6J genetic background. Ai9 female mice with ages of 8-10 weeks were used.
Wild animals	The study did not involve wild animals.
Field-collected samples	The study did not involve samples collected from the field.
Ethics oversight	All animal experiments were approved by the Institution Animal Care and Use Committees of The University of Texas Southwestern Medical Center and were consistent with local, state and federal regulations as applicable.

Note that full information on the approval of the study protocol must also be provided in the manuscript.

Human research participants

Policy information about studies involving human research participants

Population characteristics	*Describe the covariate-relevant population characteristics of the human research participants (e.g. age, gender, genotypic information, past and current diagnosis and treatment categories). If you filled out the behavioural & social sciences study design questions and have nothing to add here, write "See above."*
Recruitment	*Describe how participants were recruited. Outline any potential self-selection bias or other biases that may be present and how these are likely to impact results.*
Ethics oversight	*Identify the organization(s) that approved the study protocol.*

Note that full information on the approval of the study protocol must also be provided in the manuscript.

Clinical data

Policy information about clinical studies

All manuscripts should comply with the ICMJE guidelines for publication of clinical research and a completed CONSORT checklist must be included with all submissions.

Clinical trial registration	*Provide the trial registration number from ClinicalTrials.gov or an equivalent agency.*
Study protocol	*Note where the full trial protocol can be accessed OR if not available, explain why.*
Data collection	*Describe the settings and locales of data collection, noting the time periods of recruitment and data collection.*
Outcomes	*Describe how you pre-defined primary and secondary outcome measures and how you assessed these measures.*

ChIP-seq

Data deposition

☐ Confirm that both raw and final processed data have been deposited in a public database such as GEO.

☐ Confirm that you have deposited or provided access to graph files (e.g. BED files) for the called peaks.

Data access links *May remain private before publication.*	*For "Initial submission" or "Revised version" documents, provide reviewer access links. For your "Final submission" document, provide a link to the deposited data.*
Files in database submission	*Provide a list of all files available in the database submission.*
Genome browser session (e.g. UCSC)	*Provide a link to an anonymized genome browser session for "Initial submission" and "Revised version" documents only, to enable peer review. Write "no longer applicable" for "Final submission" documents.*

Methodology

Replicates	*Describe the experimental replicates, specifying number, type and replicate agreement.*
Sequencing depth	*Describe the sequencing depth for each experiment, providing the total number of reads, uniquely mapped reads, length of reads and whether they were paired- or single-end.*
Antibodies	*Describe the antibodies used for the ChIP-seq experiments; as applicable, provide supplier name, catalog number, clone name, and lot number.*
Peak calling parameters	*Specify the command line program and parameters used for read mapping and peak calling, including the ChIP, control and index files used.*
Data quality	*Describe the methods used to ensure data quality in full detail, including how many peaks are at FDR 5% and above 5-fold enrichment.*

Software

Describe the software used to collect and analyze the ChIP-seq data. For custom code that has been deposited into a community repository, provide accession details.

Flow Cytometry

Plots

Confirm that:

☒ The axis labels state the marker and fluorochrome used (e.g. CD4-FITC).

☒ The axis scales are clearly visible. Include numbers along axes only for bottom left plot of group (a 'group' is an analysis of identical markers).

☒ All plots are contour plots with outliers or pseudocolor plots.

☒ A numerical value for number of cells or percentage (with statistics) is provided.

Methodology

Sample preparation

For hepatocyte isolation, two-step collagenase perfusion was executed as described before Briefly, mice were anesthetized by isofluorane and fixed. Perfusion was started with liver perfusion medium (Thermo Fisher Scientific, 17701038) for 7-10 min, then switched to liver digestion medium (Thermo Fisher Scientific, 17703034) for another 7–10 min. The liver was collected into a plate containing 10 mL of liver digestion medium and cut to release the hepatocytes. Then the released hepatocytes were collected and washed with ice-cold hepatocyte wash medium (Thermo Fisher Scientific, 17704024) via low speed centrifugation (50xg) for 5 minutes. The supernatant was decanted and the pellet was re-suspended with ice hold hepatocyte wash medium. The cell suspension was passed through 100 µM filter into a new tube. The hepatocyte-cell suspension was washed twice with ice cold hepatocyte wash medium and and once with 1X PBS via centrifugation (50xg) for 5 minutes. Afterwards, the hepatocytes were further isolated by straining through a 100µm filter and using low speed (50xg) centrifugation for 5 minutes, the supernatant was removed and the re-suspended hepatocytes were analyzed by FACS Aria II SORP machine (BD Biosciences).

For isolation and staining of spleen cell types, the removed spleen was minced up by a sterile blade and homogenized in 250 µL of 1X digestion medium (45 units/µL Collagenase I, 25 units/µL DNAse I and 30 units/µL Hyaluronidase). The spleen solution was transferred into a 15 mL tube that contained 5-10 mL of 1X digestion medium. Next, the spleen solution was filtered using a 70 µm filter and washed once with 1X PBS. A cell pellet was obtained by centrifuging for 5 min at the speed of 300xg at 4 degree. The supernatant was removed and the cell pellet was resuspended in 2 mL of 1X RBC lysis buffer (BioLegend, 420301) and incubated on ice for 5 min. After incubation, 4 mL of cell staining buffer (BioLegend) was added to stop RBC lysis. The solution was centrifuged again at 300xg for 5 min to obtain a cell pellet. The single cells were resuspended in cell staining buffer and added into flow tubes that contained antibodies (100 µL total volume). The cells were incubated with antibodies for 20 min in the dark at 4 degree. The stained cells were washed twice with 1 mL 1X PBS, then resuspended in 500 µL 1X PBS for flow cytometry analysis. The antibodies used were Pacific Blue anti-mouse CD45 (BioLegend, 103126), Alexa Fluor 488 anti-mouse/human CD11b (BioLegend, 101217), Alexa Fluor 647 anti-mouse CD19 (BioLegend, 115522) and PerCP-Cyanine5.5 Anti-Mouse CD3e (145-2C11) (Tonbo Biosciences, 65-0031). Ghost Dye Red 780 (Tonbo Biosciences, 13-0865-T500) was used to discriminate live cells. The spleen cells were analyzed by LSRForessa SORP machine (BD Biosciences).

For isolation and staining of lung cell types, isolated lungs were minced up by a sterile blade and then transferred into 15 mL tube that contained 10 mL 2X digestion medium (90 units/µL Collagenase I, 50 units/µL DNAse I and 60 units/µL Hyaluronidase) and incubated at 37 °C for 1h with shaking. After incubation, any remaining lung tissue was homogenized. The following steps were similar to the spleen protocol described above. The antibodies here used were Pacific Blue anti-mouse CD45 (BioLegend, 103126), Alexa Fluor 488 anti-mouse CD31 (BioLegend, 102414) and Alexa Fluor 647 anti-mouse CD326 (Ep-CAM) (BioLegend, 118212). Ghost Dye Red 780 (Tonbo Biosciences, 13-0865-T500) was used to discriminate live cells. The lung cells were analyzed by the LSRForessa SORP machine (BD Biosciences).

Instrument

FACS Aria II SORP (BD Biosciences) and LSRFortessa SORP (BD Biosciences)

Software

Data collection: BD FACSDiva software version 8.0.1 (BD LSRFortessa);
Data analysis: FLOWJO software version 7.6 (FLOWJO)

Cell population abundance

We used tdTomato mice to evaluate tissue specific gene editing efficiency (Cre mediated) via detecting the tdTomato mean fluorescence intensity.

Gating strategy

Gates for Td-Tom+ in cell types were drawn based on control mice. Gating strategy were provided in Figure S16, S17 and S18.

☒ Tick this box to confirm that a figure exemplifying the gating strategy is provided in the Supplementary Information.

Magnetic resonance imaging

Experimental design

Design type

Indicate task or resting state; event-related or block design.

Design specifications

Specify the number of blocks, trials or experimental units per session and/or subject, and specify the length of each trial or block (if trials are blocked) and interval between trials.

Behavioral performance measures

State number and/or type of variables recorded (e.g. correct button press, response time) and what statistics were used

Behavioral performance measures

to establish that the subjects were performing the task as expected (e.g. mean, range, and/or standard deviation across subjects).

Acquisition

Imaging type(s)

Specify: functional, structural, diffusion, perfusion.

Field strength

Specify in Tesla

Sequence & imaging parameters

Specify the pulse sequence type (gradient echo, spin echo, etc.), imaging type (EPI, spiral, etc.), field of view, matrix size, slice thickness, orientation and TE/TR/flip angle.

Area of acquisition

State whether a whole brain scan was used OR define the area of acquisition, describing how the region was determined.

Diffusion MRI ☐ Used ☐ Not used

Preprocessing

Preprocessing software

Provide detail on software version and revision number and on specific parameters (model/functions, brain extraction, segmentation, smoothing kernel size, etc.).

Normalization

If data were normalized/standardized, describe the approach(es): specify linear or non-linear and define image types used for transformation OR indicate that data were not normalized and explain rationale for lack of normalization.

Normalization template

Describe the template used for normalization/transformation, specifying subject space or group standardized space (e.g. original Talairach, MNI305, ICBM152) OR indicate that the data were not normalized.

Noise and artifact removal

Describe your procedure(s) for artifact and structured noise removal, specifying motion parameters, tissue signals and physiological signals (heart rate, respiration).

Volume censoring

Define your software and/or method and criteria for volume censoring, and state the extent of such censoring.

Statistical modeling & inference

Model type and settings

Specify type (mass univariate, multivariate, RSA, predictive, etc.) and describe essential details of the model at the first and second levels (e.g. fixed, random or mixed effects; drift or auto-correlation).

Effect(s) tested

Define precise effect in terms of the task or stimulus conditions instead of psychological concepts and indicate whether ANOVA or factorial designs were used.

Specify type of analysis: ☐ Whole brain ☐ ROI-based ☐ Both

Statistic type for inference
(See Eklund et al. 2016)

Specify voxel-wise or cluster-wise and report all relevant parameters for cluster-wise methods.

Correction

Describe the type of correction and how it is obtained for multiple comparisons (e.g. FWE, FDR, permutation or Monte Carlo).

Models & analysis

n/a	Involved in the study
☐	☐ Functional and/or effective connectivity
☐	☐ Graph analysis
☐	☐ Multivariate modeling or predictive analysis

Functional and/or effective connectivity

Report the measures of dependence used and the model details (e.g. Pearson correlation, partial correlation, mutual information).

Graph analysis

Report the dependent variable and connectivity measure, specifying weighted graph or binarized graph, subject- or group-level, and the global and/or node summaries used (e.g. clustering coefficient, efficiency, etc.).

Multivariate modeling and predictive analysis

Specify independent variables, features extraction and dimension reduction, model, training and evaluation metrics.